Evaluation of brilliance, fire, and scintillation in round brilliant gemstones

Jose Sasian, FELLOW SPIE
University of Arizona
College of Optical Sciences
1630 East University Boulevard
Tucson, Arizona 85721
E-mail: jose.sasian@optics.arizona.edu

Jason Quick
Jacob Sheffield
American Gem Society Laboratories
8917 West Sahara Avenue
Las Vegas, Nevada 89117

James Caudill
American Gem Society Advanced Instruments
8881 West Sahara Avenue
Las Vegas, Nevada 89117

Peter Yantzer
American Gem Society Laboratories
8917 West Sahara Avenue
Las Vegas, Nevada 89117

Abstract. We discuss several illumination effects in gemstones and present maps to evaluate them. The matrices and tilt views of these maps permit one to find the stones that perform best in terms of illumination properties. By using the concepts of the main cutter's line, and the anti-cutter's line, the problem of finding the best stones is reduced by one dimension in the cutter's space. For the first time it is clearly shown why the Tolkowsky cut, and other cuts adjacent to it along the main cutter's line, is one of the best round brilliant cuts. The maps we introduce are a valuable educational tool, provide a basis for gemstone grading, and are useful in the jewelry industry to assess gemstone performance.
[DOI: 10.1117/1.2769018]

Subject terms: gemstone evaluation; gemstone grading; gemstone brilliance; gemstone fire; gemstone scintillation; gemstone cuts; round brilliant; gemstones; diamond cuts; diamonds.

Paper 060668R received Aug. 28, 2006; revised manuscript received Feb. 16, 2007; accepted for publication Apr. 10, 2007; published online Oct. 1, 2007.

1 Introduction

Craftsmanship of gemstones that produce appealing illumination effects has been an endeavor of the gem cutting industry throughout its history. Early gem cutters found that by properly designing and cutting a gem, especially clear diamonds, it was possible to capture light from above the gem and redirect it to the eyes of an observer. Gems are produced with a variety of cuts that comprise a plurality of planar surfaces called facets. The top facets form the crown and the bottom facets form the pavilion of the stone. The facets themselves are polygonal in their boundary. Facets in the crown capture light and facets in the pavilion reflect light by total internal reflection. This light capturing and redirection function makes a gem appear illuminated and there are several illumination effects produced that make a stone appealing. The main illumination effects are brilliance, fire, and scintillation. There is a limited set of cuts that favor the simultaneous presence of these effects that produce what is known in the trade as the life of a gemstone. Defining and quantifying brilliance, fire, and scintillation is relevant in the gem cutting industry where gem grading schemes are important for establishing value to gemstones and for informing the consumer.

When a beam of light enters a gemstone it is split and partitioned by the stone facets into a plurality of beams that are totally internally reflected and then refracted out of the stone. The refracted beams, through Fresnel splitting, create second and higher-order generations of beams that in turn are refracted out of the stone. Each beam generation carries less and less energy according to the Fresnel coefficients, to light absorption in the bulk of the gemstone material, or to light scattering by material inclusions. Light that exits the gemstone may reach the eyes of an observer creating a plurality of illumination effects that significantly impact the appearance of the gemstone. Among the most important and long-recognized[1] effects are gem brilliance, gem fire, gem scintillation, and gem leakage. Historically there have been several definitions of these effects that capture their essence. For example, brilliance refers to the ability of a stone to redirect light to the eyes of an observer so that the gem's crown appears illuminated. The effect of fire refers to the rainbow-like colors with which light exits a gem's facet as seen by an observer. Fire occurs because white light entering or exiting a stone is dispersed into its constituent colors. The effect of scintillation refers to flashes of light, white or colored light, that are produced when the gem, the observer, or the illumination source move. Scintillation is a dynamic and rich effect. The effect of leakage refers to light that exits the stone through the gem pavilion rather than through the crown and may not contribute positively to the gemstone appeal.

A primary goal in gem cutting is to maximize the carat weight of a given stone to be cut; however, recently there has been an emphasis in also maximizing the illumination appeal of gems. The illumination effects produced by gems have been traditionally evaluated with the unaided eye and with the aid of magnifiers. The first device to be recognized as an effective tool to aid in the cutting of stones is the

0091-3286/2007/$25.00 © 2007 SPIE

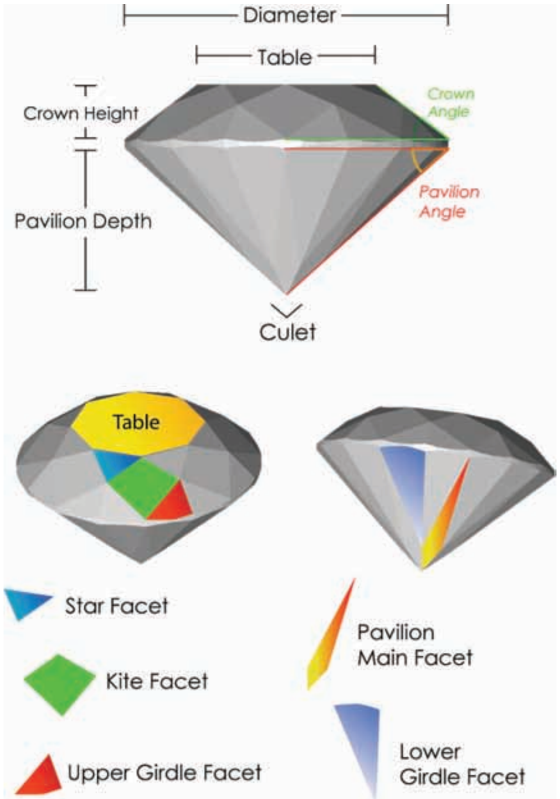

Fig. 1 Nomenclature of the round brilliant cut.

FireScope®, which was invented in Japan in 1984[2] and designed to judge brilliancy of precious stones. It is a simple device that uses a small cap painted internally red, a diffused white light source, and 10X eyepiece. Other devices for gemstone evaluation have been invented such as the Gilbertson[3] instrument, designed to provide information about gemstone symmetry and brilliance, and the Angular Spectrum Evaluation Tool (ASET)[4] device, designed to show critical directions from which a gem captures light.

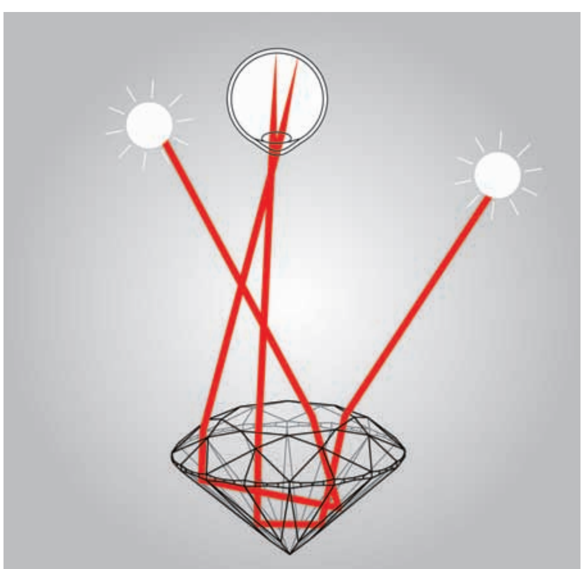

Fig. 2 Light rays can enter the gem and be redirected to the eye from different directions.

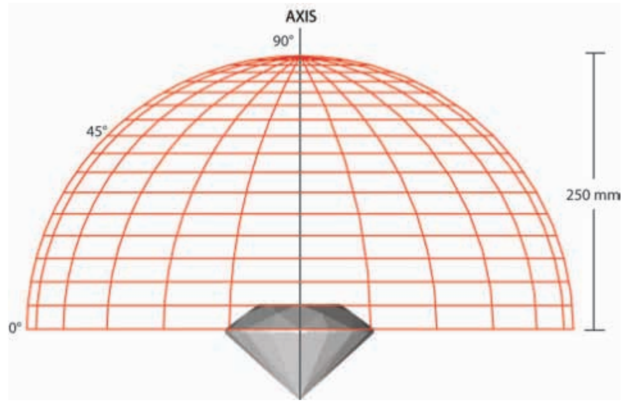

Fig. 3 Nomenclature to indicate ray directions. Normal to the gem table (the axis of the gem) is 90 deg and parallel to the table is 0 deg.

Previous studies[1,5–8] have been fruitful in understanding illumination effects in gemstones but have been limited in scope due to the lack of computing power. The development of nonsequential ray tracing software, commercial and company-proprietary, along with the ability to represent digitally and in detail the geometry of a given gemstone has resulted in the ability to model and evaluate gemstones with significant realism. For example, it is possible to design gems in a computer (GemCad[9]), model their appearance under different lighting conditions (DiamCalc[10]), and trace rays to extract other useful information (ASAP,[11] Fred,[12] LightTools,[13] TracePro,[14] and ZEMAX[15]). Given the ability for modeling gems in a computer there have been some interesting and useful studies of the round brilliant diamond as performed by the Gemological Institute of America[16,17] and Moscow State University.[18,19] Recently there has also been progress in understanding the illumina-

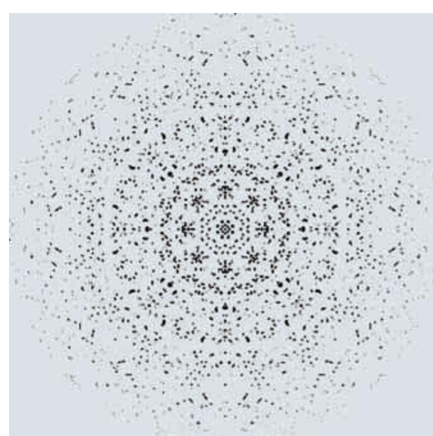

Fig. 4 Angular spectrum of a round brilliant as projected in the hemisphere. Each dot represents a ray direction that can make a virtual facet appear illuminated. Several ray refractions, including the primary, are included.

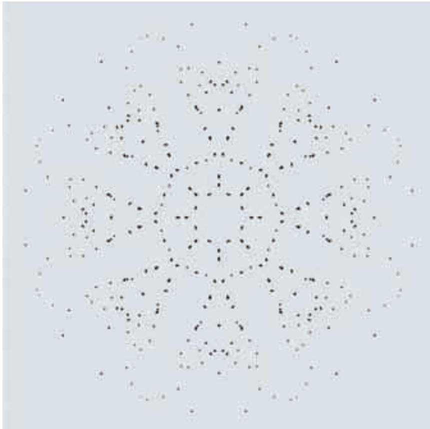

Fig. 5 Angular spectrum of a round brilliant as projected in the hemisphere. Only the primary refraction is displayed.

tion effects in gemstones,[4,20–22] in improving the cutting of stones to exacting dimensions, and in development of better tools for gem cut metrology.[23,24]

In view of this progress, there is a renewed interest in the gemstone industry for grading gems based on their performance (illumination attributes) rather than in cut proportions as has primarily been done for many decades. A grading scheme based on illumination performance requires characterization approaches that can quantify the light handling abilities of gems. The American Gem Society has been engaged in producing a simple, consistent, and realistic approach to the optical testing and characterization of gemstones, which is the subject of this paper. The primary goals of this study are to define and evaluate the illumination attributes in gems of brilliance, fire, and scintillation. The approach uses an instrument, called the Angular Spectrum Evaluation Tool (ASET), for the direct optical testing of real gemstones, including fancy shapes, and ray tracing through virtual gemstones. The study presented here discusses the round brilliant cut. We introduce evaluation maps that include angular spectrum maps, dispersion maps, scintillation maps, and glare maps. These maps simplify the evaluation of gemstones and are a valuable educational tool.

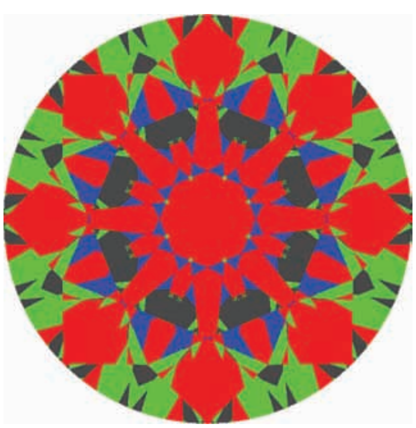

Fig. 6 ASET Map of a round brilliant gem coded by colors on the gem's crown according to angular ranges.

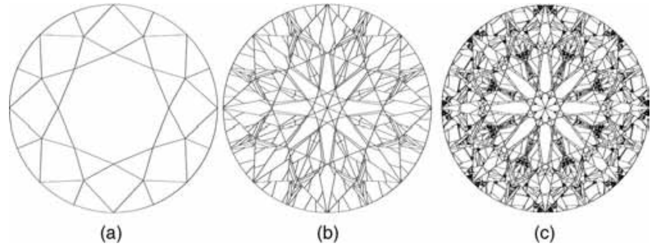

Fig. 7 (a) Cut facets, (b) virtual facets upon the primary refraction as projected on the crown in the face-up position, and (c) virtual facets upon the primary and secondary refraction in the face-up position.

2 Gemstone Nomenclature

In the jewelry industry there is a terminology to designate different portions or regions of a given gemstone and for the purpose of this paper it is appropriate to review the most significant entities as they pertain to the geometry of a gemstone. A gemstone is divided into regions comprising flat surfaces called facets as shown in Fig. 1 in cross section for the round brilliant diamond. The crown is the top portion of the stone, which in turn is divided into the table and the bezel. The bezel contains the eight star facets, eight kite facets, and sixteen upper girdle facets. The pavilion is the lower portion of the stone and is divided into the lower girdle facets, the pavilion main facets, and the culet. The girdle separates the crown and the pavilion and comprises a plurality of significantly smaller facets that are parallel to the main axis of the stone. The axis of the stone passes through the center of the culet and it is perpendicular to the table. For the case of the standard round brilliant cut diamond there are 58 facets, 33 in the crown and 25 in the pavilion.

The standard round brilliant is one out of a plurality of cut possibilities within the round shape. There are many other important cut geometries such as the emerald, princess, oval, pear, and marquise cuts, which are known in the trade as fancy cuts. Each cut has their own myriad of variations that produce different illumination effects to the observer.

3 Geometrical Angular Spectrum and Structured Illumination

One insightful approach to analyzing illumination effects in gems is to utilize the concept of geometrical angular spectrum. The angular spectrum can be considered as a gem signature and intrinsically carries the cut proportions. Here

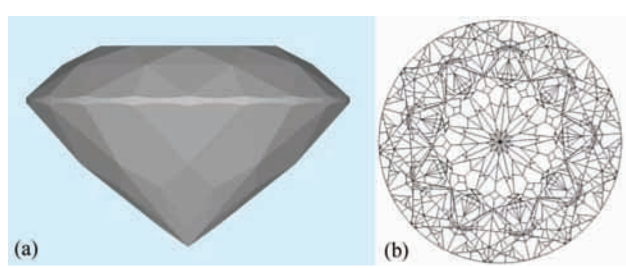

Fig. 8 The Gabrielle cut (a) and its virtual facets (b) upon the primary refraction.

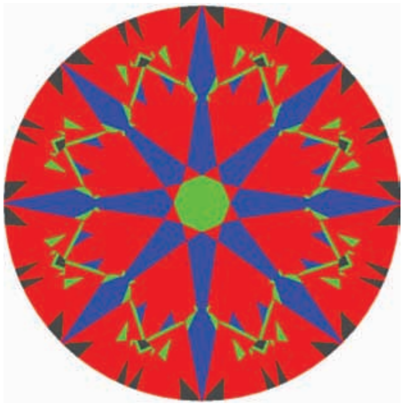

Fig. 9 ASET Map of the Tolkowsky cut upon the primary refraction. Gray areas represent light leakage.

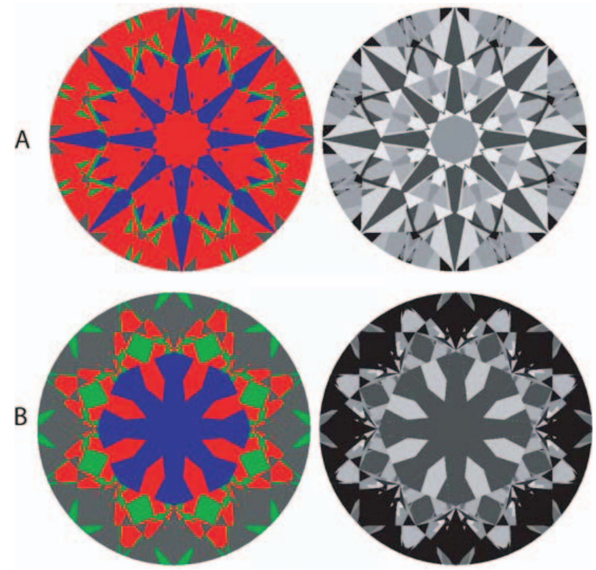

Fig. 10 (a) ASET (left) and gray-scale (right) map of a round brilliant cut that is brilliant, and (b) ASET (left) and gray-scale (right) map of a cut that shows little brilliance.

angular spectrum refers to the set of ray angle directions that can make the facets of a gem appear illuminated. For a given position of a gem in relation to an observer there is a set of directions with which rays can enter a gem and be directed to the observer's eye. An entering ray will be first split into two due to Fresnel reflection. The reflected ray will be considered as contributing to glare if it reaches the observer's eye. The refracted ray will be internally reflected until it is refracted out of the gem and will contribute to brilliance and fire if it reaches the observer's eye. This ray upon exiting will be split and the resulting reflected ray will continue to be refracted and split. Thus the angular spectrum of a gem contains ray directions corresponding to a first generation of rays split only once upon exiting the gem (known as primary refraction), a second generation of rays split twice (known as secondary refraction), and other-higher ray generations according to the number of ray splits. The first ray generation will contain most of the energy of the original entering rays. Successive ray generations will contain significantly less energy. For the case of diamond that has an index of refraction of 2.4 about 83% of the energy remains in the refracted ray and about 17% in the reflected ray. Materials with a lower index of refraction will contain more energy in the refracted ray. Thus the primary refraction accounts significantly for the appearance of a gem.

The appearance of a gemstone depends not only on a gem's cut geometry, which determines the angular spectrum, but on the illumination conditions. For example, diffuse illumination will favor brilliance and localized illumination, such as spot lighting, will favor fire and flash scintillation. Regardless of the illumination, each illumination distribution will have associated an angular spectrum and the product of the angular spectrums of the illumination and the gemstone will determine the stone's appearance. The concept of angular spectrum is helpful to decouple the contributions to a gem's appearance from the illumination conditions and its cut. It would be possible to arrange the illumination conditions to make many gems appear with the attributes of brilliance, fire, and scintillation. In practice the illumination conditions are not ideal and therefore under the average illumination conditions, only a limited set of cuts will exhibit those illumination attributes in a significant manner.

It can be stated that the visual appeal of a gemstone is related to the variety of illumination effects that it can produce. A gemstone that appears evenly illuminated with no fire or scintillation attributes has little appeal. To produce brilliance, fire, and scintillation the illumination must be structured and this can be achieved in three manners. The first is by the illumination conditions of the environment where the stone is observed; the second is by the partial obscuration of the gem's angular spectrum by the observer, and the third manner is by the intrinsic properties of the cut. Structured lighting is a key concept for understanding and producing illumination effects in gemstones and it is emphasized in this paper.

4 Angular Spectrum Acquisition and Display

Figure 2 shows the eye of an observer, a gemstone, and two rays that reach the eye of the observer upon the primary refraction. Each ray has a particular direction and the set of directions of rays that reach the observer's eye constitutes

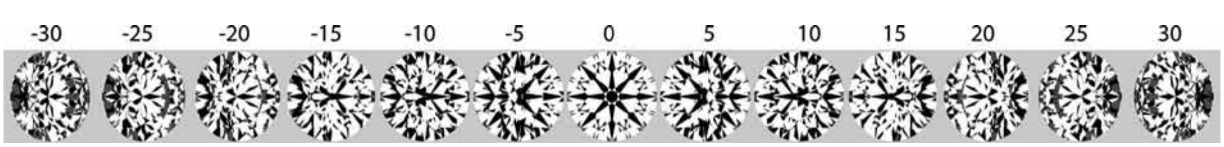

Fig. 11 The phenomenon of dynamic contrast shown in a series of tilt positions ranging from −30 to 30 deg in 5-deg intervals.

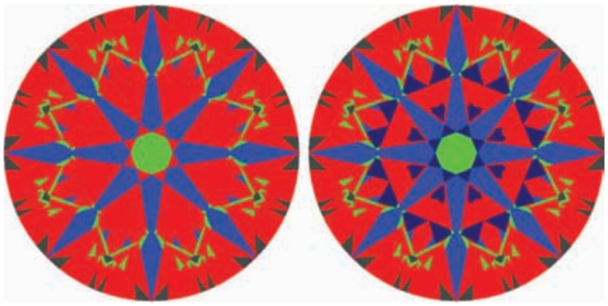

Fig. 12 ASET maps of the Tolkowsky cut with 30 (left) and 40 (right) deg of obscuration (blues) for the high angles. The 40-deg ASET map shows the added blue regions with a darker hue.

the angular spectrum of the primary refraction. The distance at which the eye is positioned with respect to the stone is set to 250 mm from the stone table and along the axis of the stone. This observation geometry is called the face-up position. Other observation geometries that involve tilting the stone are called tilt positions. A hemisphere of radius 250 mm with its center in the girdle plane is a useful reference to indicate ray directions. The axis of the stone passes through the center of the hemisphere and ray directions are measured with respect to the plane of the table. Thus a direction of 90 deg coincides with the axis of the stone and hemisphere as shown in Fig. 3.

One way to acquire the angular spectrum of a gem is through computer modeling and ray tracing. Rather than forward illuminating the gem, a reverse ray trace starting at the observer's eye will indicate the ray directions that actually can bring light to the observer's eye. If these ray directions are projected into the hemisphere, then a 2-D map as shown in Fig. 4 can be produced. This map shows the ray directions or angles that can contribute to brilliance and fire. In this 2-D map each dot represents a particular ray direction. The map includes several generations of ray splits and shows the richness of the angular spectrum given the Fresnel ray split. In comparison, Fig. 5 shows the angular spectrum contributed only by the primary refraction. In this later case there is a one-to-one mapping between the direction and the point where a ray exits the gem's crown in its path to the observer's eye.

Although reverse ray tracing can easily display a precise representation of the angular spectrum in the hemisphere, it is more insightful to actually show regions in the gem's crown that contribute to specific angular spectrum ranges. We have defined three angular ranges in relation to the surface of the table in the stone crown: low angles are from 0 to 45 deg, medium angles from 45 to 75 deg, and high angles from 75 to 90 deg. Figure 6 shows the appearance of a gem when the angular ranges as projected in the gem's crown are coded by color (green low angles, red medium angles, and blue high angles). Gray regions represent light that leaks through the pavilion and therefore do not contribute to brilliance or fire. This representation of the angular spectrum by ranges and zones on a gem's crown is useful because it directly relates ray directions to crown zones and therefore can be easily interpreted. We call this graphical representation of the angular spectrum an ASET map.

The choice of the angular ranges to acquire the angular spectrum reflects practical considerations. The high angles range (blues) is set from 75 to 90 deg because the head of an average observer can block this angular range. Thus upon the face-up position the blues represent areas in a gemstone that may not receive light due to the obscuration of the observer's head. The medium angles (reds) are set from 45 to 75 deg. This choice comes from four considerations: first is the knowledge of the angular spectrum of gemstones that are brilliant, second is the fact that observation of gemstones is naturally done with light arriving either from the back or above the head of the observer, third is the structured lighting that is created in the gemstone due to the obscuration of the head and body when the stone is in movement, and fourth is that in realisitic environments illumination frequently occurs at angles greater than 45 deg. The low angles range (greens) is set from 0 to 45 deg as it does not contribute significantly to brilliance or structured lighting. There is some simplification in the ranges selected that intends to account for common illumination and observation conditions. Increasing the number of angular ranges would provide more information at the expense of practical simplification. For example, ASET maps with variations in the tone of the three main colors according to further angular subdivision can add useful information. The three angular ranges in elevation are deemed to be appropriate for the purposes of the characterization approach presented in this paper. Given the eightfold symmetry of the round brilliant cut there is no need to further subdivide the angular ranges in the hemisphere with respect to azimuth. Some fancy cuts with reduced symmetry, however, would require further subdivision of the hemisphere to acquire more detailed information about their angular spectrum.

5 Illumination Effects

The main goal of this paper is the evaluation of the illumination effects of brilliance, fire, and scintillation. However, a full understanding of these desirable effects requires taking into consideration other effects. Therefore in this section we review the illumination effects of virtual facets, brilliance, contrast, fire, scintillation, leakage, and glare, and introduce maps that permit their evaluation. The structured lighting in these maps is conveyed by the spatial distribution and variety of colors in the maps as commented

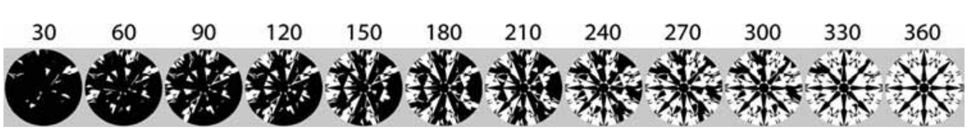

Fig. 13 Brilliance of a round brilliant stone as the illumination over the hemisphere increases in 30-deg sectors. Note that by 180 deg the crown is substantially illuminated and exhibits positive contrast properties.

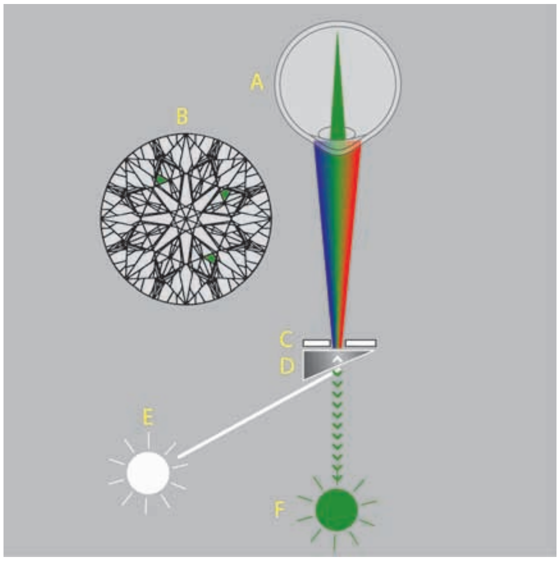

Fig. 14 How light dispersion and the clipping of the eye pupil can produce a colored appearance of a small facet. (A) eye, (B) virtual facet appearance, (C) small aperture, (D) prism, (E) light source, and (F) virtual source image.

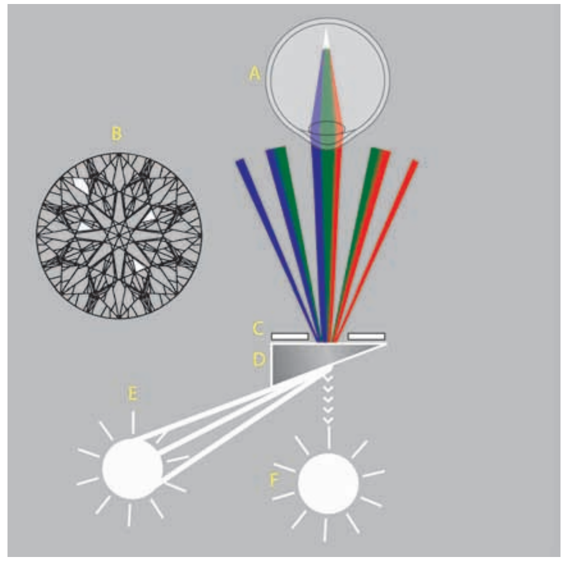

Fig. 16 Rays from a large source can recombine to produce a non-colored, white appearance of a facet. (A) eye, (B) virtual facet appearance, (C) small aperture, (D) prism, (E) light source, and (F) virtual source image.

below. By design, the bezel in a gemstone has more structure than the table and therefore the bezel exhibits more illumination effects.

5.1 *Virtual Facets*

The observation of a gemstone reveals that its appearance consists of many more facets than the actual number of cut facets. This occurs because as a beam of light enters a gemstone it is divided into a plurality of beams resulting from the projection of the entering beam on the gemstone facets as shown in Fig. 7. These perceived facets are known as virtual facets and their number depends on the number of actual facets the stone has and on the number of times light is partitioned as it propagates in the stone. Within the round shape there are cut geometries that include more facets than the standard round brilliant cut such as the Gabrielle® cut. This cut is shown in a solid view and with its virtual facets upon the primary refraction in Fig. 8. The size and distribution of the virtual facets have an impact on the visual appeal of a stone. If the size of the virtual facets approaches the limit of the eye's resolution then fire and flash scintillation will tend to appear as pinpoint events. If the size of the facets is several times larger than the eye's resolution then the effect of facet interplay can be observed. This effect is desirable and consists of the sudden change of appearance of groups of alternate facets becoming dark, illuminated, or colored. Facet interplay is reminiscent of the sudden changes in pattern produced by a kaleidoscope when it is in movement.

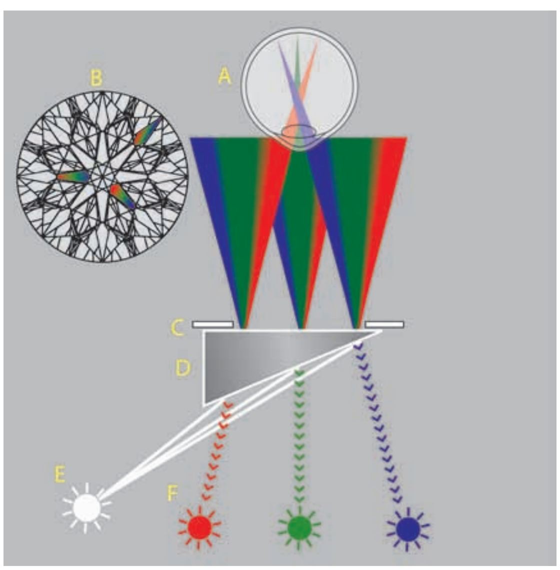

Fig. 15 A large facet can appear multicolored since it can redirect to the eye dispersed light from different locations in the facet. (A) eye, (B) virtual facet appearance, (C) large aperture, (D) prism, (E) light source, and (F) virtual source images.

Upon secondary refraction, further beam partitioning takes place and the virtual facets become smaller, as is also shown in Fig. 7. The small virtual facets upon secondary and higher-order refractions contribute to pinpoint fire and scintillation. The first refraction mostly contributes large virtual facets, which are key in producing facet interplay. Thus the primary refraction is the most significant because of the amount of light it carries and the size of the virtual facets.

5.2 *Gem Brilliance*

Gemstone brilliance refers to the ability of a stone to appear illuminated to an observer. For this to occur light must be directed from the virtual facets to the observer's eyes. In this paper we measure the illumination effect of brilliance by the observed area of the crown that can direct light from the medium angles to the observer's eye. Figure 9 shows the primary angular spectrum of the Tolkowsky cut as projected in a stone crown. For this cut, 20.5% of the crown is

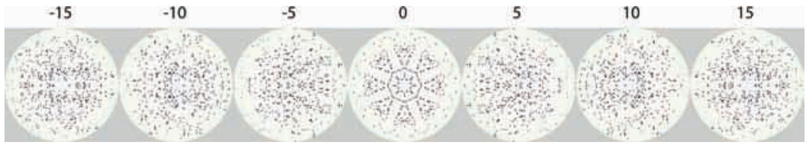

Fig. 17 Angular spectrum of a gemstone as projected in the hemisphere upon −15, −10, −5, 0.0, 5, 10, and 15 deg tilts. This sequence shows that upon tilting a stone the probability of intersecting a source by the angular spectrum is essentially one.

illuminated with light from the high angles (blues), 67.0% with light from the medium angles (reds), 7.2% with light from the low angles (greens), and 5.3% of the light is not redirected to the observer's eyes due to leakage.

Under broad diffuse illumination the crown of a stone may substantially appear evenly illuminated. However, if the illumination environment is structured and comprises several sources of white light that have an appreciable angular subtend, of a few degrees to a few tens of degrees, then some virtual facets would appear white and bright while others would appear translucent or dim. When a virtual facet is illuminated it appears to the observer as if it is a light source by itself.

For understanding the illumination appearance of a gem it is useful to think of a gem's facets and their optical projections, the virtual facets, as a collection of tiny prisms that direct light to an observer's eyes. Thus brilliance in this paper is defined as the percentage (by area) of such tiny prisms that can direct light to the observer's eyes. This definition is simple and does not intend to account for obliquity factors that could be included to account for differences in the relative position of facets or illumination conditions. For example, in typical illumination scenarios the relative intensity of light provided by light sources varies significantly from place to place. This makes the inclusion of obliquity factors substantially irrelevant. In addition, the definition is congruent with the intuitive idea that something brilliant is an object that can direct light to an observer's eye. Thus a gem is said to have the attribute of brilliance if it can direct light to the observer's eyes. Effectively, a brilliant gem can be equated with a structured light source. Figure 10 shows the ASET and gray-scale maps of a round brilliant cut that is deemed to be brilliant and one that is not. The perception of brilliance also depends on the background as it is discussed next.

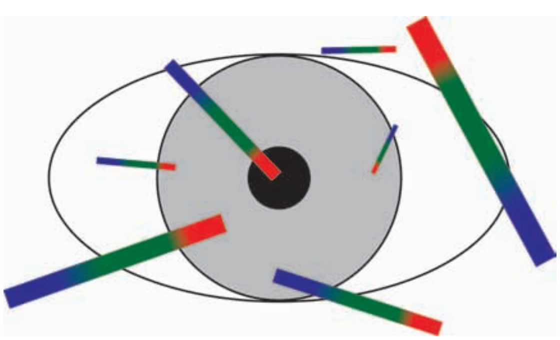

Fig. 18 The bigger the chromatic flares are, the larger the probability is of being captured and clipped by the eye's pupil.

5.3 *Gem Contrast*

The high angular range as represented by blue color in an ASET map indicates the zones in a stone crown that are not illuminated due to the obscuration of the observer's head. This obscuration produces what is known in the trade as gem contrast.[19,20] In proper amount and distribution, contrast creates structured lighting that enhances brilliance, fire, and scintillation. Contrast can be a detrimental effect if it is significantly localized. Too little contrast results in a stone appearance lacking variety under broad diffused illumination. Too much contrast results in a stone that lacks brilliance. The combination of positive contrast characteristics and brilliance properties in a gemstone is known as contrast brilliance.

When a gemstone is in movement the contrast pattern changes in form. This effect is called dynamic contrast and adds substantial appeal to the appearance of a stone as statically shown in Fig. 11 with a series of tilt maps ranging from −30 to 30 deg in 5-deg intervals.

Contrast, as represented by the blue region in the ASET maps, is acquired by blocking a cone of 30 deg in the angular spectrum. Additional information about contrast is obtained by increasing the angular spectrum obscuration to 40 deg. This increased obscuration represents having the observer looking closer at the stone, closer than 250 mm, and it is used to critically evaluate the contrast properties of gemstones in the face-up position. Figure 12 shows the ASET maps for the Tolkowsky cut with 30 and 40 deg of obscuration. The fact that the Tolkowsky cut retains a well-balanced contrast pattern in these two views indicates superiority in creating structured lighting. Thus characterizing gem contrast is essential in assessing the visual appeal of gemstones.

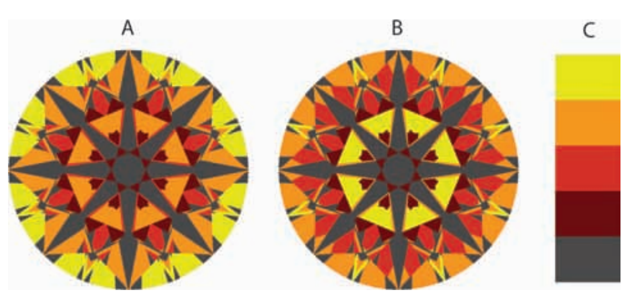

Fig. 19 (a) Forward fire map, (b) reverse fire map, and (c) key: gray indicates obscured, low-angle light or leakage. Dark orange indicates a linear dispersion of 2.0 mm or less at the eye of the observer (forward map) or at the source (reverse map). Orange is dispersion between 2.0 mm and 4.2 mm, light orange is dispersion between 4.2 mm and 6.4 mm, and yellow is dispersion larger than 6.4 mm for the chosen wavelengths of 420 and 620 nm.

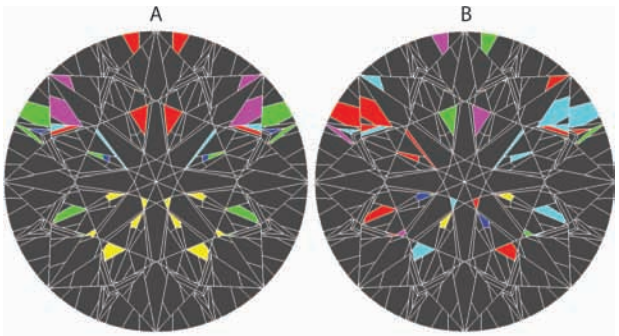

Fig. 20 Scintillation maps of a round brilliant with (a) concentric illumination and (b) sector illumination. Concentric illumination shows how the virtual facets are illuminated as a source scans radially the hemisphere. Sector illumination shows how the virtual facets are illuminated as a source scans in azimuth the hemisphere.

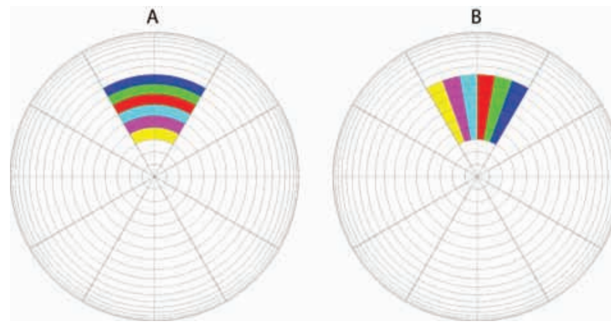

Fig. 21 Illumination key in the hemisphere with (a) concentric illumination over the medium angles, and (b) sector illumination over the medium angles. The colors used are red, green, blue, cyan, magenta, and yellow.

An alternate view to contrast properties is shown in Fig. 13 where the hemisphere increases its illumination as the azimuth range is increased from zero to 360 deg in 30-deg increments and upon the face-up position.

5.4 *Gem Fire*

The phenomenon of fire is one of the most appealing effects in transparent gemstones. Under favorable conditions fire makes individual facets appear fully colored with the rainbow hues.[25,26] Fire inherently occurs due to the light dispersion upon refraction as light enters and exits a stone. Three factors determine the amount of fire perceived from a facet, namely, the angular dispersion of light upon refraction from the gemstone, the angular subtend of the source, and the angular subtend of the eye's pupil in relation to the facet.

To best observe fire it is required to have a localized source of light so that its angular subtend is much smaller than the angular dispersion produced by the gem facet, essentially a point source. As different colored rays arrive to the eye from a facet, some of them enter the eye's pupil and others are blocked producing a colored appearance of the facet as shown in Fig. 14. In this process the boundary of the eye's pupil plays a critical role in obstructing portions of the spectrum to achieve the colored facet appearance. At 250 mm of distance and considering the dispersion of diamond, which is on the order of 0.044, wavelengths at 420 and 620 nm can be linearly spaced up to several millimeters by a gem. Depending on the illumination conditions and the age of the observer, the human pupil size can range from about 2 to 8 mm in size. Therefore there is some variability on the amount of fire perceived by different observers in different illumination conditions.

Relative to the eye's position, the angular subtend of a given facet determines the appearance of the facet. If the subtend of the facet is small, then only one color would be observed across the facet. As the angular subtend of the facet increases, more colors would be observed, until finally the entire spectrum would be seen. Essentially, the eye would be observing the source at different lateral locations depending on the color as shown in Fig. 15. The facet size would be large enough to permit the eye to see the source at those different locations. However, gem facets are typically small so that in the presence of fire they appear substantially with a single color.

As the angular size of the source increases from a small fraction of a degree to a few degrees the color saturation will decrease. Intermediate colors such as green will disappear first, then only blue and red will be observed, and finally no colors will be observed. In this process of increasing the source size, ray overlap from different locations in the source takes place, washing out the colored appearance of the facet as shown in Fig. 16.

Modeling of gem fire can be done by assuming specific localized illumination scenarios such as spot lighting or chandelier illumination. However, gem evaluation may favor certain cuts that perform better in those specific illumination conditions. The approach to characterize fire followed in this paper is based on the observation that the angular spectrum of most realistic cuts is rich. When a gemstone is in movement, for example, tilted back and forth, its angular spectrum scans the hemisphere, resulting in essentially a probability of one to intersect a given localized light source. This observation is illustrated in Fig. 17, which shows the angular spectrum of a gemstone that has been tilted in the range of ±15 deg with respect to the face-up position. The practical meaning of this observation is that for evaluating fire one can factor out the illumination conditions. Thus, our evaluation of fire is independent of the source distribution. Appendix A provides further support with a study of the angular spectrum as a function of stone cut parameters.

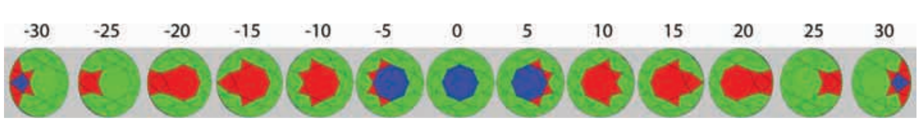

Fig. 22 Glare maps of a round brilliant showing directions in the hemisphere that can contribute glare. The maps are in tilt positions ranging from −30 to 30 deg in 5-deg intervals.

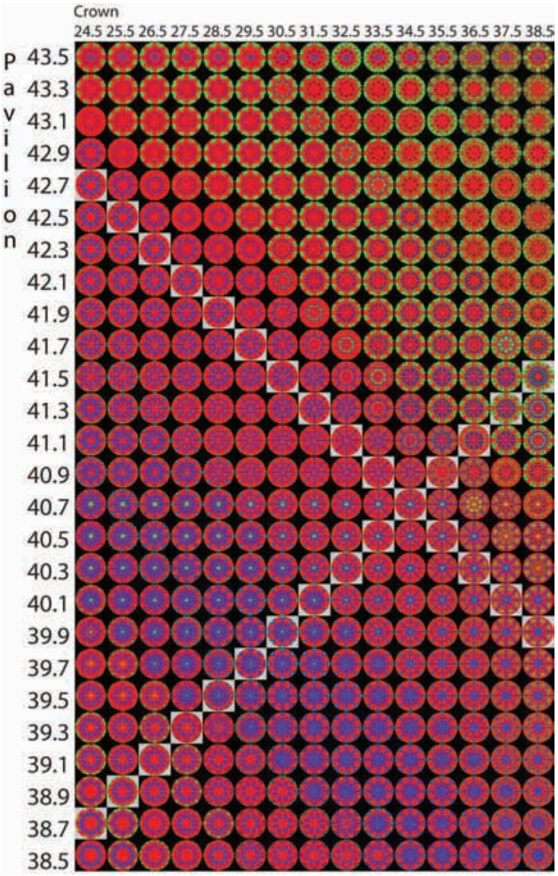

Fig. 23 A matrix of ASET maps as a function of crown and pavilion angles upon primary refraction. The highlighted diagonal lines represent the main cutter's line (slope of −1) and the anti-cutter's line (slope of +1). Note that illumination properties are similar along lines parallel to the main cutter's line. (High-resolution image available online only. [URL: http://dx.doi.org/10.1117/1.2769018.1])

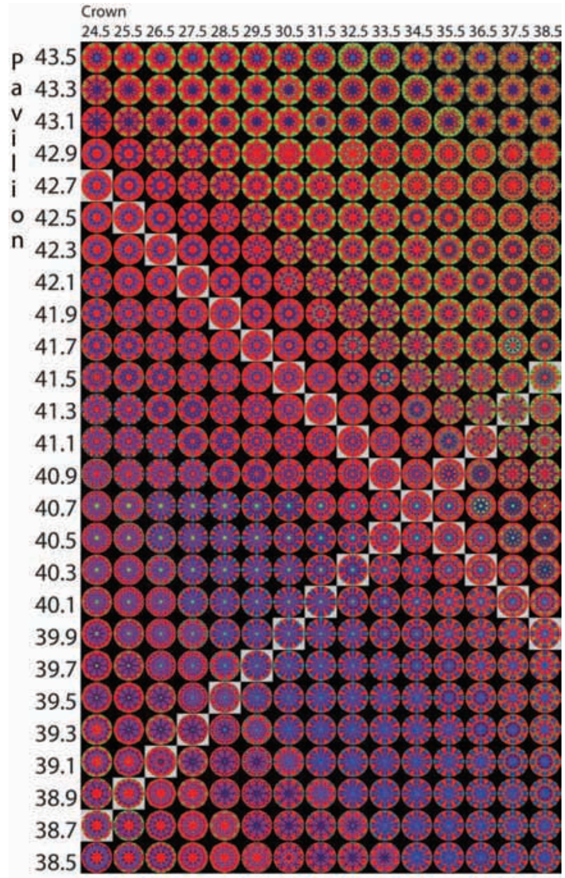

Fig. 24 ASET matrix with 40 deg of obscuration upon primary refraction. (High-resolution image available online only. [URL: http://dx.doi.org/10.1117/1.2769018.2])

Then, the next important factor in the production of fire is the amount of dispersion that rays from facets in a gem's crown have. Gemstones at a distance of 250 mm possess barely enough dispersion (on the order of millimeters) to separate the light colors across the observer's pupil. The amount of dispersion from each virtual facet is a significant measure of fire. The larger the dispersion from a facet, the higher the probability will be that the eye's pupil will clip dispersed rays to produce a colored appearance as shown in Fig. 18. When there is a larger amount of dispersion, the color perceived will be purer (more color saturation) but with a decrease in intensity. The decrease in color intensity is not a concern due to the relatively high brightness of localized sources that can produce fire.

Figure 19 shows what we call a fire map, which indicates the potential of a stone to produce fire. It is actually a dispersion map, coded by colors, that indicates the amount of dispersion that a white-light ray will undergo in reaching the observer's eye at a distance of 250 mm in the face-up position. Dark orange indicates a linear dispersion of 2.0 mm or less at the eye of the observer. Orange is dispersion between 2.0 mm and 4.2 mm, light orange is dispersion between 4.2 mm and 6.4 mm, and yellow is dispersion larger than 6.4 mm for the chosen wavelengths of 420 and 620 nm. Fire maps are produced by tracing two rays per crown position at different wavelengths and noting the amount of dispersion. Two fire maps, for each stone geometry, can be produced depending on the use of reverse (from the eye to the source) or forward (from the source to the eye) ray tracing. Forward fire maps, produced in the observer's space, show the potential to observe fire. Reverse fire maps, produced in the source space, show the potential to observe a source. The dispersion in the reverse and forward fire maps is related by the anamorphic magnification associated to the prism corresponding to each virtual facet.

There are other factors that can determine fire in a gemstone, as for example the amount of light from higher-order refractions that coincide with the primary refraction upon exiting the gemstone. The structured lighting that results from dynamic contrast and the inherent light scrambling inside the gemstone are other factors that count. However, the fire maps upon primary or higher-order refractions (those that result from Fresnel ray split) convey significantly the fire potential of a stone and are a valuable tool for assessing gem fire.

5.5 *Gem Scintillation*

In the presence of brilliance and fire the most appealing effect is gem scintillation. In this effect the fire pattern

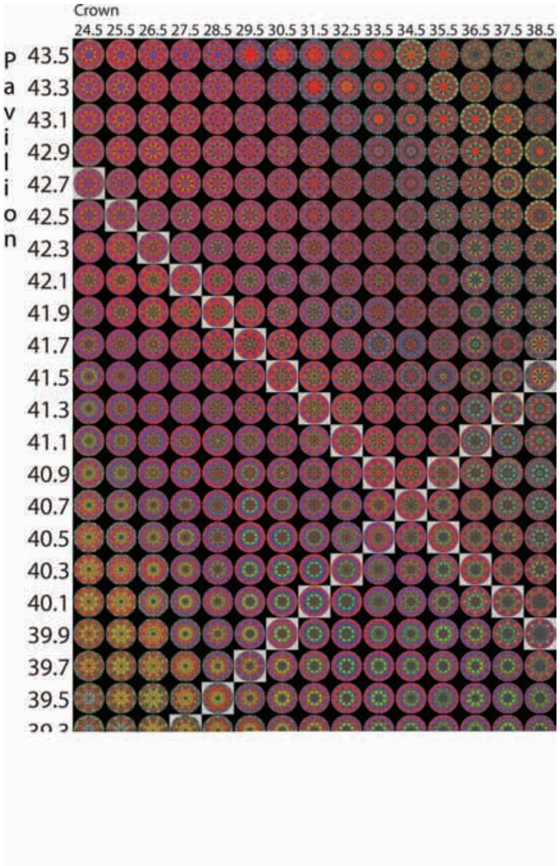

Fig. 25 ASET matrix upon secondary refraction. (High-resolution image available online only. [URL: http://dx.doi.org/10.1117/1.2769018.3])

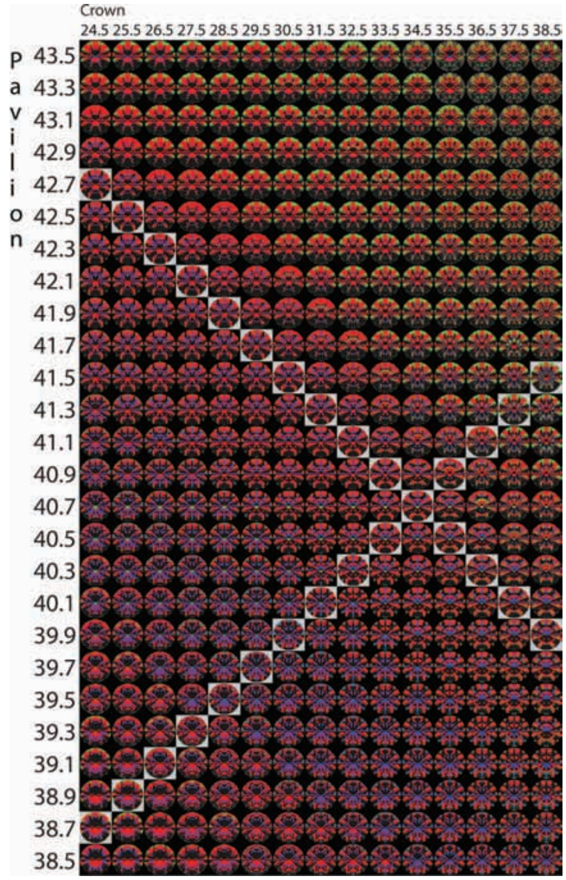

Fig. 26 ASET matrix produced with one half of the illumination hemisphere. (High-resolution image available online only. [URL: http://dx.doi.org/10.1117/1.2769018.4])

changes dynamically and flashes of white light are perceived across the crown of the stone. Thus there are two major scintillation effects, fire and flash scintillation. To observe them it is required that the stone, the observer, or the illumination conditions be in movement. Typically the observer tilts the stone back and forth to observe scintillation and naturally optimizes for the direction that maximizes scintillation. Without brilliance, as defined in this paper, there cannot be fire since no light can be brought to the observer's eyes. Without fire there cannot be fire scintillation as defined by the change of fire pattern. Flash scintillation can occur without fire scintillation and it is due to light sources not small enough in angular subtend to produce fire, or to the inability of a stone to sufficiently disperse light for a given position of the observer. White diffused illumination will wash out both scintillation effects. Sources that subtend a small angle will contribute more to produce a flash effect, the rapid turn on and off of the light from a given facet, than sources that subtend larger angles. Thus fire scintillation is more vivid than flash scintillation.

The amount of gem scintillation perceived is linked to the brilliance and fire of a stone. However, scintillation strongly depends on the change of illumination conditions. This change is primarily produced on purpose by the movement of the stone as it is admired. The effects on scintillation due to the stone movement in turn can be enhanced according to the intrinsic light scrambling properties of the stone. These light scrambling properties of a stone are the third mechanism to produce structured lighting. In this paper we define the light scrambling properties of a stone as its ability to mix or scramble its angular spectrum as it is projected into the stone crown. In particular, attention is paid to the scrambling of the medium angular range or reds in the ASET maps.

Figure 20 shows what we call scintillation maps. These maps are generated with light reaching the observer's eye in the face-up position from the medium angles, 45 to 75 deg, in the hemisphere and in a 60-deg sector as shown in Fig. 21. They are presented in six colors (red, green, blue, cyan, magenta, and yellow) to further subdivide the medium angles into regions that are concentric arc circles or truncated pie sections. The interpretation of the scintillation maps is different than the ASET maps. Recall that in the ASET maps colors indicate the ray directions that can make a stone crown appear illuminated. The scintillation maps represent the change in illumination of the crown as a light source scans, in azimuth or radially, the medium angles in the hemisphere. A stone deemed to substantially scramble light would appear with the colors well distributed over its crown in the scintillation map view. In Fig. 20 the size and form of the virtual facets is clearly shown as well as the illumination distribution over the crown of the gem. Thus a scintillation map conveys information about

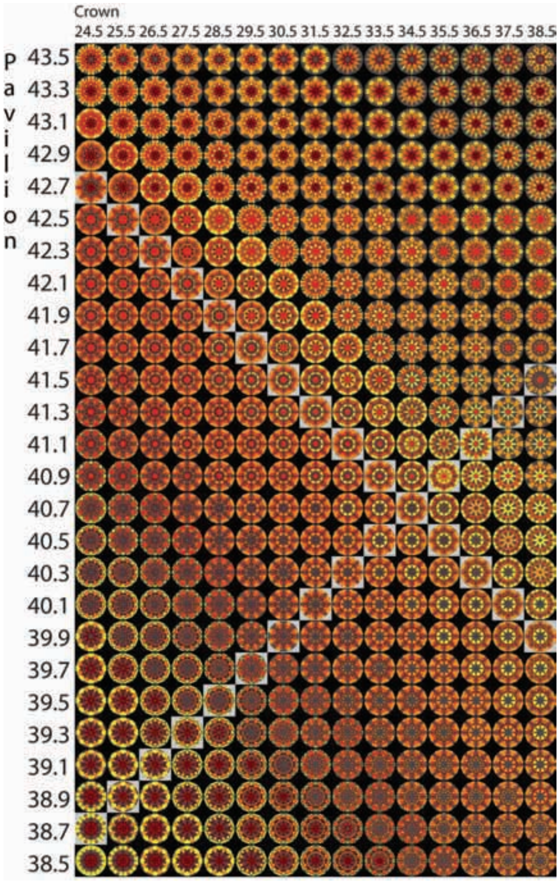

Fig. 27 Matrix of reverse fire maps upon primary refraction. (High-resolution image available online only. [URL: http://dx.doi.org/10.1117/1.2769018.5])

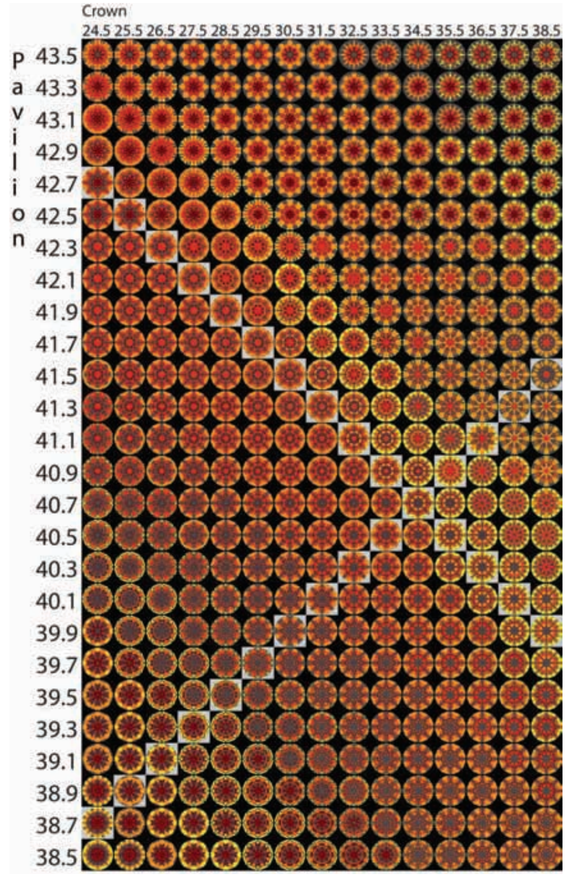

Fig. 28 Matrix of forward fire maps upon primary refraction. (High-resolution image available online only. [URL: http://dx.doi.org/10.1117/1.2769018.6])

the size and form of the virtual facets and about the intrinsic light scrambling properties of a gem, and hints at how a stone would exhibit scintillation.

5.6 *Gem Leakage*

Gem leakage refers to areas in the pavilion where total internal reflection does not occur. Consequently and depending on the light source, the light intensity from leaky regions may not be as intense as in other regions in the stone. In addition, in stones that are mounted in pronged mounts it is possible for light to enter through the pavilion and reach the observer's eye by exiting though the crown. Upon secondary refraction, leakage areas can also contribute to fire and scintillation given that localized sources are bright. Leakage can be considered a detrimental effect, though it is possible that small amounts of leakage that are well distributed may add variety to the illumination effects in a positive manner.

5.7 *Gem Glare*

Gem glare results from the reflection of a light source on the surface of crown facets. This light does not enter the stone and hides the appreciation of the main illumination effects that are perceived inside the stone. Figure 22 shows a series of glare maps that indicate, upon the face-up position and tilt positions, the directions in the hemisphere that can produce glare. Glare maps with significant glare from the medium angles (reds) are deemed undesirable; they correspond to stones with shallower crown angles.

6 Map Matrices

In the previous section we have introduced several maps that are useful in evaluating and comparing gemstones. This section provides matrices of maps as a function of the crown and pavilion angles for a given table size of a standard round brilliant cut. In this study the table size is 53%. The maps give an ample view of the trade-offs in the cut space as commented for each map. The horizontal axis corresponds to the crown angle ranging from 24.5 deg (left) to 38.5 deg (right) with 1.0-deg intervals. The vertical axis corresponds to the pavilion angle ranging from 38.5 deg (bottom) to 43.5 deg (top) with 0.2-deg intervals. The maps are generated with the primary refraction except as indicated for some ASET and fire maps. It will become apparent that the matrices show certain important trends in illumination properties. The Tolkowsky cut is a reference cut and is located at P41.7/C34.5 where P41.7 indicates a pavilion angle of 41.7 deg and C34.5 a crown angle of 34.5 deg.

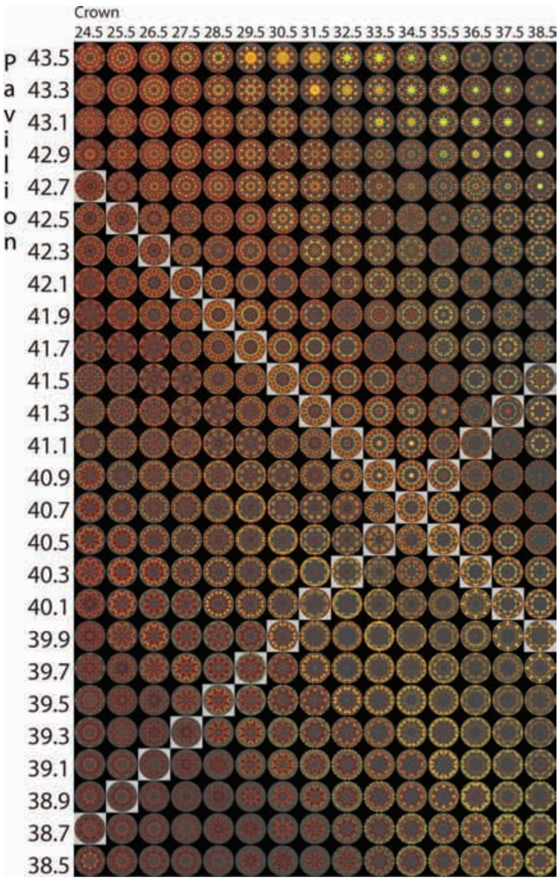

Fig. 29 Matrix of reverse fire maps upon secondary refraction. (High-resolution image available online only. [URL: http://dx.doi.org/10.1117/1.2769018.7])

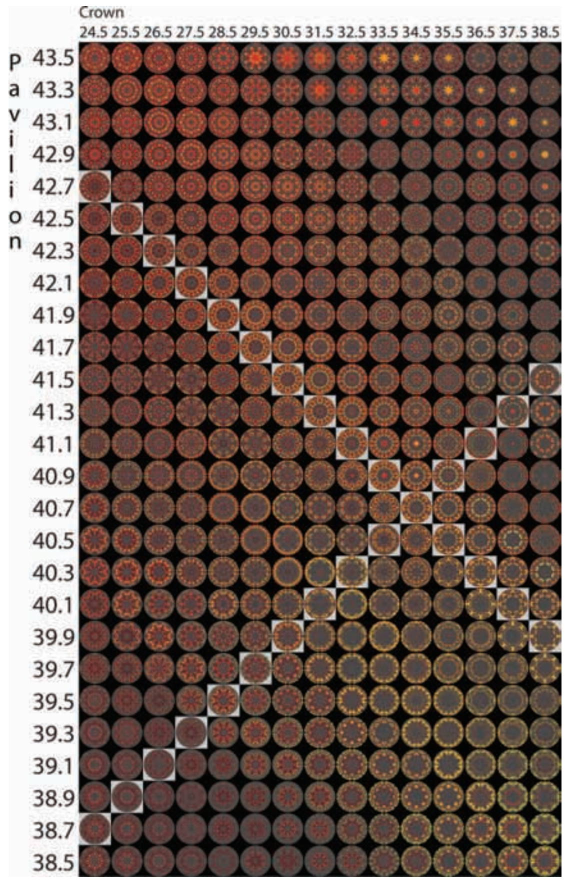

Fig. 30 Matrix of forward fire maps upon secondary refraction. (High-resolution image available online only. [URL: http://dx.doi.org/10.1117/1.2769018.8])

6.1 *ASET Maps*

Figure 23 shows a matrix of standard ASET maps (30 deg of obscuration) in the face-up position for the round brilliant cut. The matrix shows that there is a trade-off between crown angle and pavilion angle. That is, a crown change of 1 deg can be traded-off by a pavilion angle change of about 0.2 deg to maintain the same properties to within some limits. As far as brilliance is concerned this trade-off has been known in the industry for some time. What is little known is that the trade-off exists even for other properties as is shown in the matrices describing other illumination effects. Given the steps in the vertical and horizontal axis the stones appear to have similar properties along lines running at 45 deg (slope of -1) from top to bottom. The 45 deg (slope of -1) line passing by the Tolkowsky cut is called the main cutter's line. This line gives insight to diamond cutters about how to adjust the crown angle for a given pavilion angle change and represents a trade-off in stone cutting. Other lines at 45 deg that are parallel to the main cutter's line are called cutter's lines. A line perpendicular to the main cutter's line (slope of $+1$) and that also passes by the Tolkowsky cut is called the anti-cutter's line. The recognition of the cutter's trade-off simplifies considerably the analysis of gemstones. The main differences in stone behavior within reasonable limits appear along the anti-cutter's line. Thus the cutter's trade-off reduces the analysis from an N-dimensional to an $(N-1)$-dimensional analysis. Both the main cutter's line and the anti-cutter's line are highlighted in the matrices.

The ASET maps are the most important descriptors of illumination performance given that they characterize brilliance and contrast. The maps with significant reds and some well-distributed blues are the stones that are deemed to perform the best. The stones on the lower left are brilliant but, as discussed below, suffer from some problems. One of these problems is that upon stone tilt the girdle as reflected by the pavilion appears in the table. In the extreme, these types of stones are called fish-eyes. The brilliant stones near the Tolkowsky and along the main cutter's line are the best performers. Note that the Tolkowsky cut appears to be near a boundary where the stones change properties.

Stones with significant blues in the table are called nailheads because the table appears dark due to light retroreflection and/or obscuration upon close examination. The stones with significant greens will tend to lack brilliance in the bezel and structured lighting. Some other stones have significant leakage as shown by the gray regions.

The matrix of ASET maps also supports the choice of angular ranges to subdivide the hemisphere. For example, the low angles (greens) are mainly distributed over the bezel and have a poor distribution over the crown of stones in

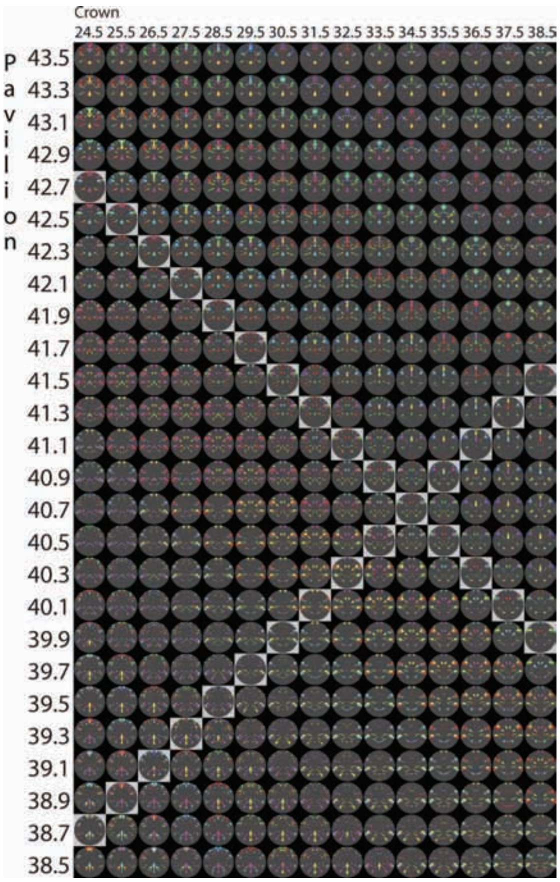

Fig. 31 Matrix of scintillation maps upon primary refraction. (High-resolution image available online only. [URL: http://dx.doi.org/10.1117/1.2769018.9])

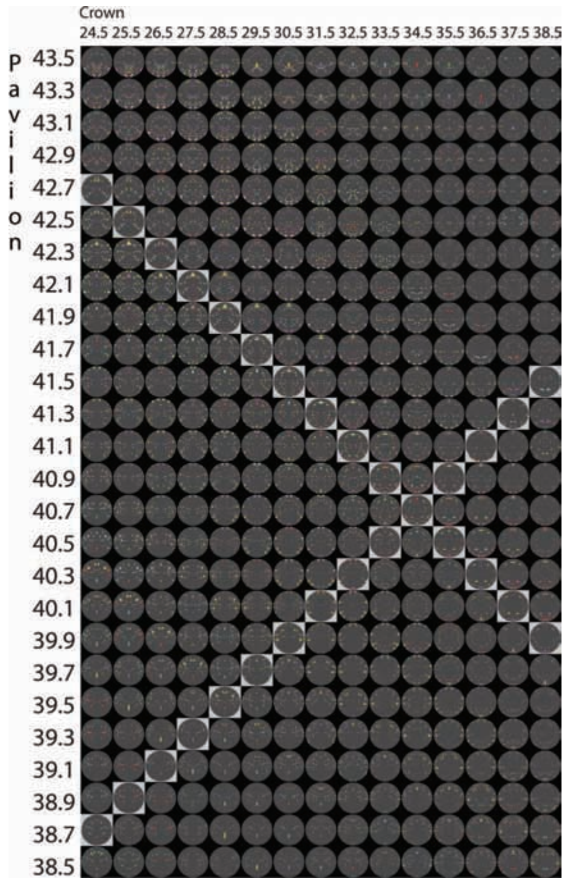

Fig. 32 Matrix of scintillation maps upon secondary refraction. (High-resolution image available online only. [URL: http://dx.doi.org/10.1117/1.2769018.10])

the matrix. The stones in the top right corner of the ASET map matrix are the ones that contribute more low-angle light. Thus low-angle light does not significantly contribute to brilliance or structured lighting. In regard to the high angle (blues), its distribution and amount can be significant; however, its angular range is essentially set by the extent of the observer's obscuration.

Figure 24 shows a matrix of ASET maps for 40 deg of obscuration, which illustrates how the contrast properties hold or change upon a closer examination of the stone. Note that the only stones that exhibit a positive contrast pattern change are the ones near the Tolkowsky cut along the main cutter's line. Other cuts like the nail-heads develop excessive contrast. Some of the cuts with no contrast remain without contrast. The ASET maps with 40 deg of obscuration also convey the structured lighting abilities of gems.

Figure 25 shows a matrix of ASET maps upon the secondary refraction. The main feature of this matrix is that it shows that cuts along the main cutter's line remain brilliant upon the secondary refraction. In addition, the contrast properties also remain positive. Stones along the anti-cutter's line change significantly in their contribution to brilliance. The shallow crown, shallow pavilion stones on the left corner are not considered brilliant upon the secondary refraction given that they contribute light from the

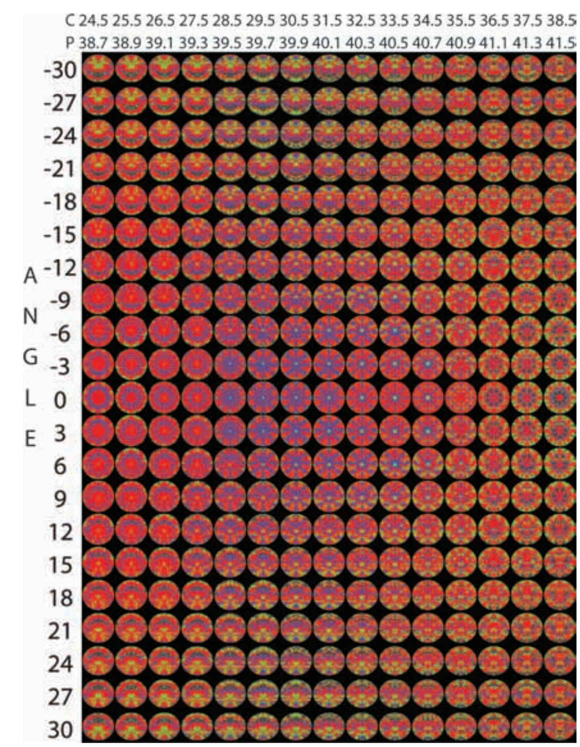

Fig. 33 Tilt view matrix of ASET maps upon primary refraction along the anti-cutter's line. (High-resolution image available online only. [URL: http://dx.doi.org/10.1117/1.2769018.11])

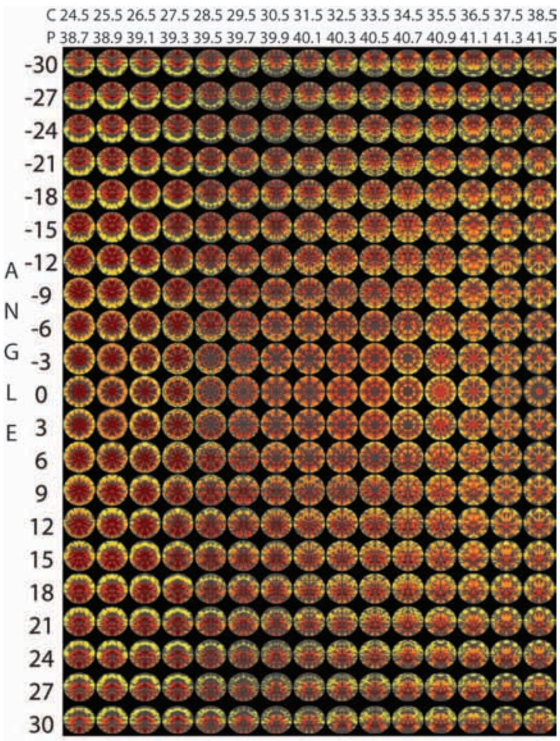

Fig. 34 Tilt view matrix of forward fire maps upon primary refraction along the anti-cutter's line. (High-resolution image available online only. [URL: http://dx.doi.org/10.1117/1.2769018.12])

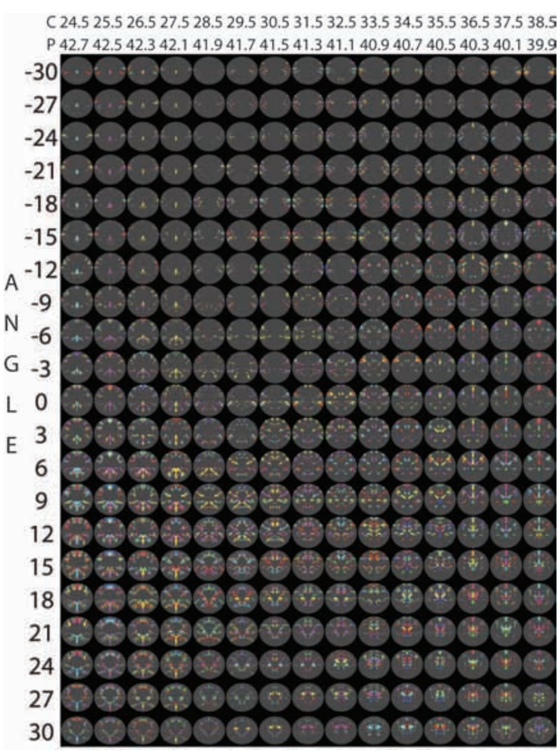

Fig. 35 Tilt view matrix of scintillation maps upon primary refraction along the anti-cutter's line (concentric illumination). (High-resolution image available online only. [URL: http://dx.doi.org/10.1117/1.2769018.13])

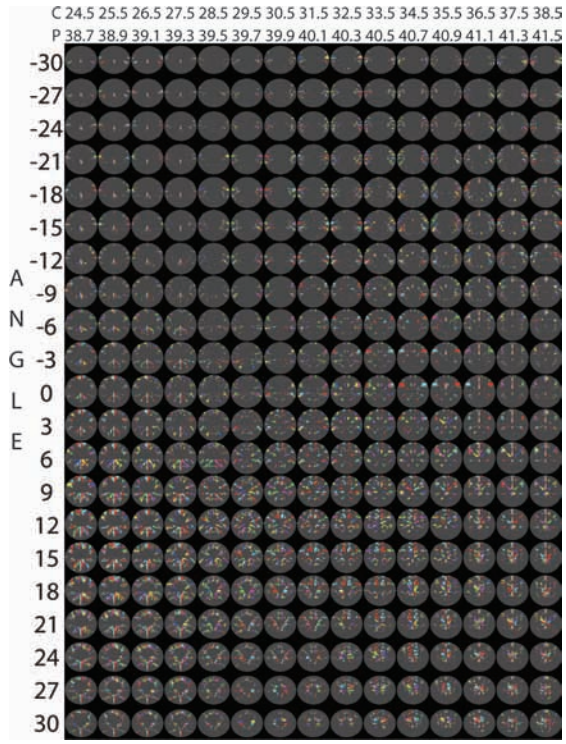

Fig. 36 Tilt view matrix of scintillation maps upon primary refraction along the anti-cutter's line (sector illumination). (High-resolution image available online only. [URL: http://dx.doi.org/10.1117/1.2769018.14])

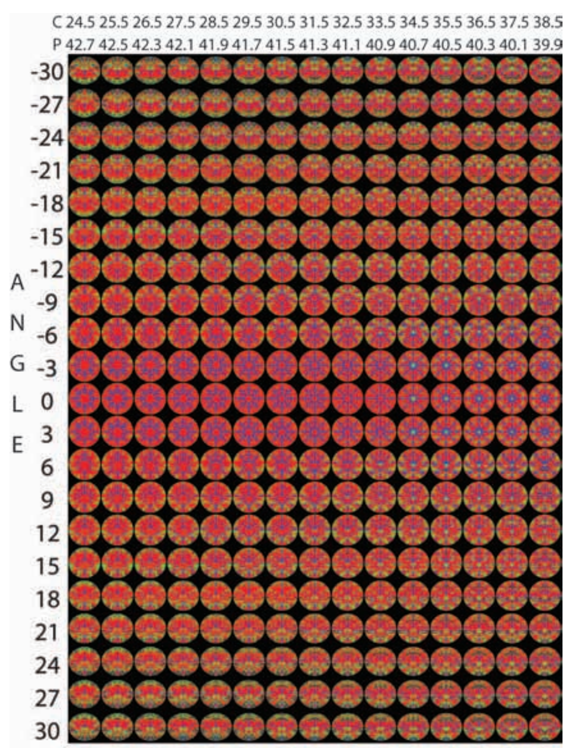

Fig. 37 Tilt view matrix of ASET maps upon primary refraction along the cutter's line. (High-resolution image available online only. [URL: http://dx.doi.org/10.1117/1.2769018.15])

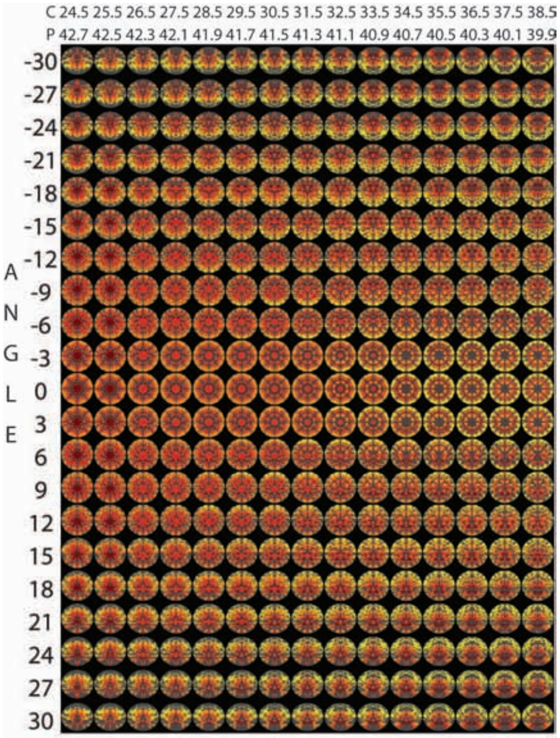

Fig. 38 Tilt view matrix of forward fire maps upon primary refraction along the cutter's line. (High-resolution image available online only. [URL: http://dx.doi.org/10.1117/1.2769018.16])

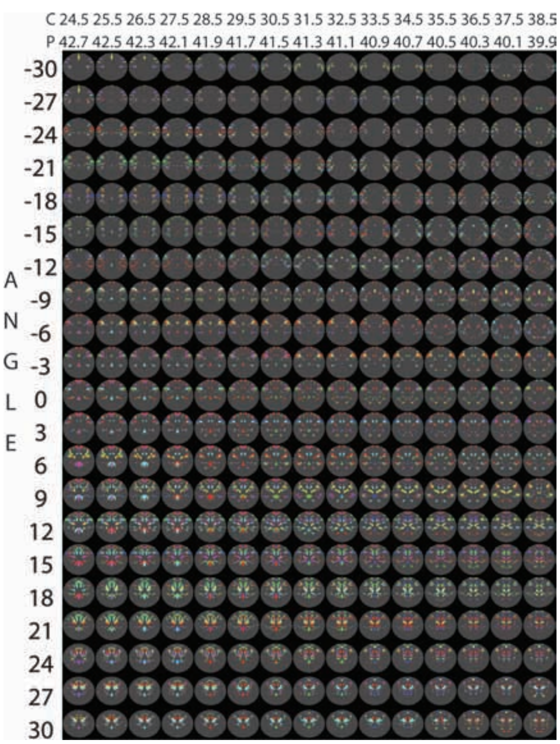

Fig. 39 Tilt view matrix of scintillation maps upon primary refraction along the cutter's line (concentric illumination). (High-resolution image available online only.
[URL: http://dx.doi.org/10.1117/1.2769018.17])

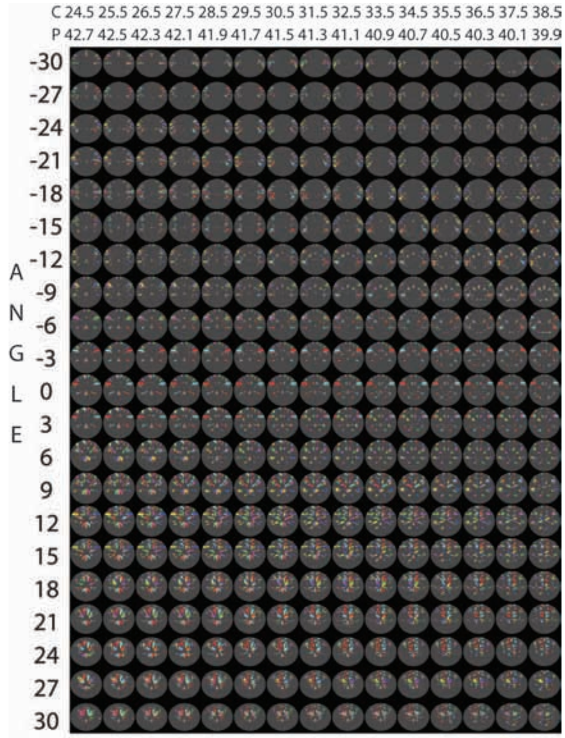

Fig. 40 Tilt view matrix of scintillation maps upon primary refraction along the cutter's line (sector illumination). (High-resolution image available online only. [URL: http://dx.doi.org/10.1117/1.2769018.18])

lower angles (greens). Note also that the pavilion-crown angle trade-off holds to a lesser extent upon the secondary refraction.

A useful modification of the ASET maps is the half-ASET map produced with half the hemisphere obscured. Figure 26 shows a matrix of half-ASET maps. Under half-hemisphere illumination the structured lighting produced by the intrinsic properties of the cut are revealed. Stones at or near the main cutter's line retain positive contrast characteristics. Other stones, as for example the shallow crown, shallow pavilion stones, exhibit a half nail-head contrast pattern and lack brilliance. The stones on the top right corner of the matrix lack brilliance in the bezel and are leaky.

6.2 *Fire Maps*

Figures 27 and 28 show matrices for reverse and forward fire maps, respectively. The reverse fire map shows the potential to observe a light source given that the chromatic flare (the spread of light into a spectrum) covers a larger area in the hemisphere, which increases the probability of intersecting a given light source. The forward fire map shows the potential to observe fire given that the larger the chromatic flare, the larger the probability is that the eye's pupil would clip and capture light from a facet. Forward fire maps are considered the main tool to assess the gem's intrinsic fire potential (without considering the source distribution and observer).

Both reverse and forward fire maps maintain the trade-off between crown and pavilion angles along the cutter's lines. The stones that exhibit significant fire are along the main cutter's line. These stones have the property of exhib-

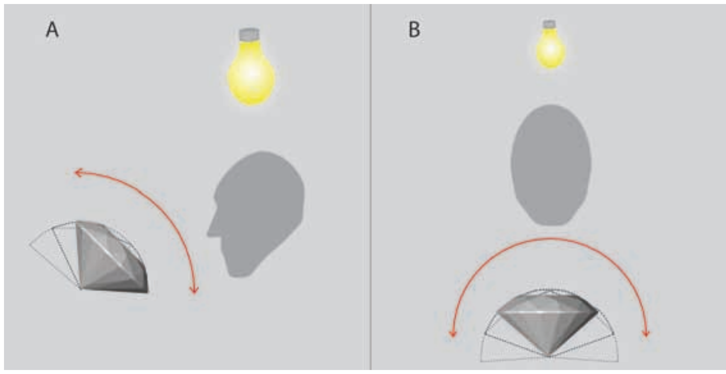

Fig. 41 (A) Forward and backward tilts in relation to the observer and source, and (B) left and right tilts in relation to the observer and source.

iting relatively high dispersion in the table. Other stones that have high dispersion are in the lower-left and top-right corners of the fire matrices. However, these stones suffer from not having high dispersion in the table.

The fire matrices show that the old diamond-cutting industry rule of increasing the crown angle to achieve more fire is not necessarily true. It only significantly applies to stones at or near the main cutter's line or about lines passing by other regions such as the left-bottom and top-right corners.

Fire results from higher dispersion and this mainly happens in the stone bezel. Table fire is rare and stones with significant bezel and table fire are considered superior. Some stones that exhibit significant fire[27] are designed with a small table to maximize the bezel area and therefore fire.

Figures 29 and 30 show some matrices for reverse and forward fire maps upon secondary refraction, respectively. The matrix for reverse fire exhibits significantly more dispersion than the matrix for forward fire. However, in both matrices the stones near or at the main cutter's line appear with significant fire potential.

6.3 *Scintillation Maps*

Figure 31 shows a scintillation matrix produced upon the face-up position. Each of the virtual facets that captures light from the hemisphere appears colored and this is termed a scintillation event. The first measure of scintillation potential is brilliance (reds in the ASET maps), given that for scintillation to occur the stone must be able to redirect light to the observer's eye. The stones that have more well-distributed scintillation events in color and over the stone's crown have the potential to produce more scintillation than stones with lesser events. For example, Fig. 31 shows that stones at or near the main cutter's line have spatially well-distributed events as compared to other stones.

Figure 32 shows a scintillation matrix upon secondary refraction. This matrix shows that the virtual facets become smaller and scintillation may appear as a pinpoint effect upon localized bright sources. Given that light upon secondary refraction is reflected more times inside the stone, the scintillation appears as more rapidly changing compared to scintillation from the primary refraction.

7 Tilt Views

Although the maps in the face-up position are a primary tool for evaluating gemstones, they do not provide sufficient information about the performance of a stone as it moves. The tilt-view matrices that we present below provide a view of the gem properties as a function of the tilt with respect to the hemisphere and the observer. The tilt views are generated by tilting the stone from −30 deg to 30 deg in 3-deg increments. Figures 33–36 show the tilt views for the round brilliant cut along the anti-cutter's line for ASET maps, forward fire maps, and scintillation maps. Figures 37–40 show the tilt views along the cutter's line. In the tilt views the Tolkowsky cut is highlighted for ease of identification.

The scintillation tilt maps are generated by tilting the stone along the symmetry line of the illuminating, truncated pie sector in the hemisphere as shown in Fig. 41. This is equivalent to tilting a stone forward and backward as it is observed. The top maps (−15 to −30 deg of tilt) in the tilt view correspond to the backward tilts, the middle map to the face-up position, and the bottom maps (+15 to +30 deg of tilt) to the forward tilts. It can be appreciated that the larger number of scintillation events occur upon the face-up position (no tilt) and forward tilts to about 15 deg. The scintillation events observed in the tilt maps correspond to

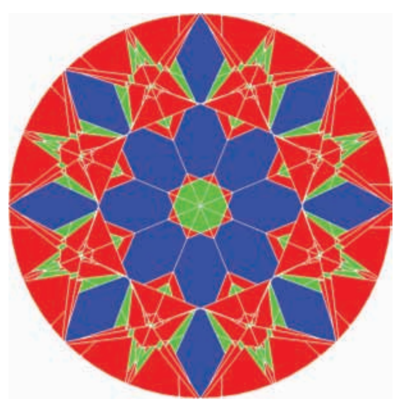

Fig. 42 Tolkowsky cut, ASET map, lower girdle facets length 60%, star facets length 35%.

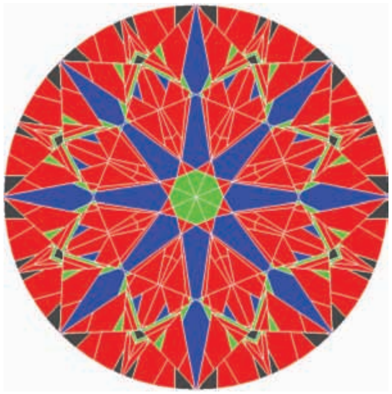

Fig. 43 Tolkowsky cut, ASET map, lower girdle facets length 80%, star facets length 50%.

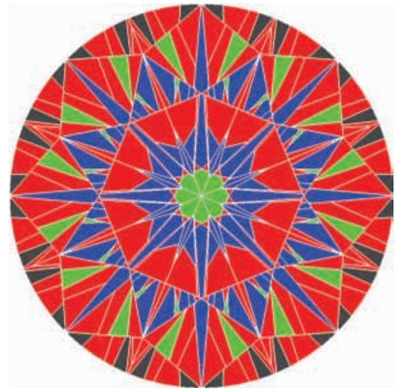

Fig. 44 Tolkowsky cut, ASET map, lower girdle facets length 90%, star facets length 50%.

the events that one would observe when the stone is tilted quickly left to right while holding it at a given forward-backward tilt position.

In the scintillation tilt maps a light source is assumed to be located above and behind the head of the observer. The exact location and size of the light source does not change qualitatively the series of scintillation events seen in the tilt view maps. These scintillation events are concentrated in the table when the stone is tilted forward, spread over the crown as the stone has less tilt, and then appear in the bezel (left and right bezel areas) as the stone is tilted backward. Thus the tilt-view scintillation maps represent in a color-coded manner what an observer would actually see in examining a stone. The number of events and their distribution in the scintillation tilt views indicate the scintillation properties of a stone.

The tilt-view ASET maps along the anti-cutter's line, Fig. 33, show that the best performers in terms of contrast and brilliance are located at the main cutter's line and possibly at the left and right adjacent lines. The tilt-view forward fire maps, Fig. 34, indicate that, in terms of fire potential, stones in the cutter's line and in the line to the right exhibit the best fire. The scintillation tilt views, Figs. 35 and 36, show that stones along the main cutter's line have the best scintillation as indicated by the number and distribution of events. Thus the cutter's trade-off and the tilt views permit one to determine the cutter's line where the best round brilliant cuts are located. These cuts are located along the main cutter's line.

The tilt views along the cutter's line, Figs. 37–40, permit one to determine which are the best stones in terms of illumination performance. The tilt-view ASET maps along the cutter's line, Fig. 37, show that the Tolkowsky cut, the two to the left (P40.9/C33.5 and P41.1/C32.5), and the one to the right (P40.5/C35.5) are the best in terms of contrast pattern and brilliance. The tilt-view, forward fire maps, Fig. 38, indicate that in terms of fire potential the stones in the main cutter's line, the Tolkowsky, and the next four stones exhibit the best fire. The scintillation tilt-view maps, Figs. 39 and 40, show that stones that exhibit the best scintillation are the last seven in the main cutter's line given the better distribution of scintillation events at tilts around the face-up position. Considering the ASET, fire, and scintillation maps the four best round brilliant stones (table 53%) are P40.9/C33.5, P40.7/C34.5 (Tolkowsky), P40.5/C35.5, and P40.3/C36.5.

For completeness of analysis Appendix A provides additional tilt matrices along the main cutter's line and anti-cutter's line.

8 The Tolkowsky Cut

Tolkowsky[1] described the reasoning that he followed to arrive at the proportions of one of the best cuts for a round brilliant. In his research he was guided by the proportions of stones that were known to exhibit superior performance. His research supported the knowledge that cutters, by trial and error, had generated over time. In his statement "…we conclude that the correct value for the pavilion angle is 40 degrees and 45 minutes and gives the most vivid fire and greatest brilliancy, and that although a greater angle would give better reflection, this would not compensate for the loss due to the corresponding reduction in dispersion" it becomes apparent that Tolkowsky noted that his cut is a compromise between brilliance and dispersive properties. In fact, contrast and scintillation are part of the overall balance. The compromise is clearly shown in the tilt views along the main cutter's line. Tolkowsky and the cut industry advocate high dispersion to achieve fire, which is consistent with our research and fire maps. From Tolkowsky's time the round brilliant cut has been improved[3] by increasing the girdle thickness, including girdle facets, reducing the culet size, and increasing the length of the lower girdle facets and star facets. Figures 42–44 show a study in lower girdle length and star facets. Figure 42 shows the old round brilliant cut with large virtual facets in the table (lower girdle facets length 60%, star facets length 35%), Fig. 43 shows the modern cut with a balanced virtual facet size that favors the effect of facet interplay (lower girdle facets length 80%, star facets length 50%), and Fig. 44 shows the round brilliant cut with thin pavilion mains (lower girdle facets length 90%, star facets length 50%).

The Tolkowsky cut and other cuts along the main cutter's line have some amount of leakage in the bezel. One way to reduce or avoid this leakage is by the technique called painting[28,29] in which the facet angle between the upper girdle facets and the kite facets is reduced. Depending on the length of the star facets, painting can have a

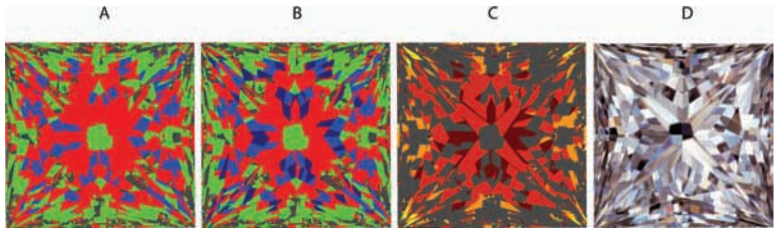

Fig. 45 (a) ASET map, (b) ASET map (40 deg of obscuration), (c) forward fire map, and (d) photograph of a high-performing princess cut.

negative impact on dispersion. Stones along the cutter's line can be painted more without negative dispersion effects.

9 Evaluation of Fancy Shape Cuts

The methodology developed to characterize illumination effects discussed below can also be applied to study fancy shape gems such as the princess and emerald cuts. Some fancy shapes have less symmetry than the eightfold symmetry of the round diamond and others more, for example, fourfold and ninefold symmetry. Therefore the angular spectrum of some fancy cuts may not be as rich as it is for the round brilliant cut and additional angular ranges in elevation and in azimuth could be necessary to sufficiently assess the illumination properties. It is also possible to have fancy cuts with richer angular spectra than the angular spectrum of round brilliants. Each fancy cut requires a study by itself. However, the maps and concepts developed in our research can still be applied for evaluating fancy cuts. For example, using our methodology we have identified a princess and an emerald cut as shown in Figs. 45 and 46 that upon actual fabrication[30,31] resulted in stones that displayed superior fire and brilliance. These cuts have not been previously known to the industry and their specifications are given in Appendix B.

10 ASET Instrument

We have developed an instrument called the Angular Spectrum Evaluation Tool (ASET) to practically evaluate gems and demonstrate results obtained by ray tracing of virtual gems. The ASET instrument is shown in Fig. 47 and consists of a stage where the gem is placed, a hemisphere carrying the colors according to angular range, a light source, and a camera. Figure 48 shows an actual photograph through the ASET of a round brilliant gem and its corresponding ray-traced computer generated view. Note the significant match between the real and virtual ASET images.

One way to observe dispersion is by creating an illumination scenario with a plurality of white sources[32] distributed over the illuminating hemisphere. The ASET instrument can be modified to display light dispersion as shown in Fig. 49. The modification requires placing a plurality of white light sources over the medium angles in the hemisphere. This is actually produced by placing a screen with pinholes in front of a light diffuser and a broad, white-light source. The angular separation of the pinholes in the screen is about the same as the angular dispersion produced by the gem. In this manner the colors produced by a single light source are not washed out by the overlap with colors from an adjacent source. However, the pinholes are still close enough to essentially always have light from a pinhole illuminating each virtual facet. An additional aperture in front of a camera serves the same function as the eye pupil in clipping colored rays. By closing or opening this aperture, more or less saturation in the colored facets can be achieved. It is not possible to directly generate fire maps. However, the colors and color saturation in the views generated are in agreement with fire maps. For example, Fig. 50 shows a sequence of photographs of a round brilliant where the clipping aperture is varied in size; the corresponding fire map is also shown. Note that the actual photographs show the crown bezel with more saturated colors. This can be explained from the higher dispersion shown in the bezel by the fire map.

11 Real Versus Virtual Gemstones

The study presented in this paper has been done in a computer using virtual gemstones that are perfect in their proportions and symmetry. Real gems are not perfect in their geometry and suffer from several problems such as facet

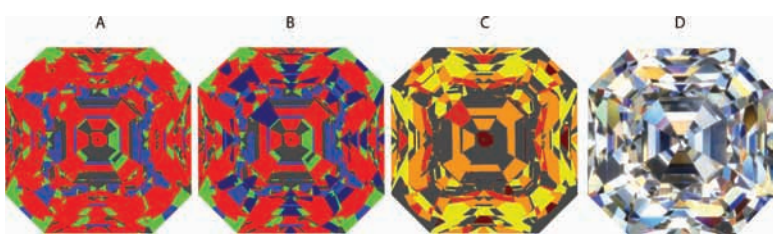

Fig. 46 (a) ASET map, (b) ASET map (40 deg of obscuration), (c) Forward fire map, and (d) photograph of a high-performing emerald cut.

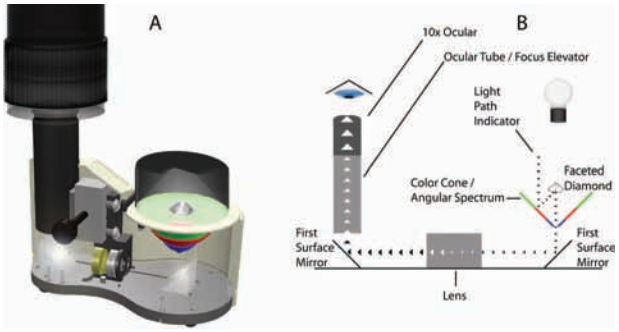

Fig. 47 (a) ASET instrument and (b) schematic diagram.

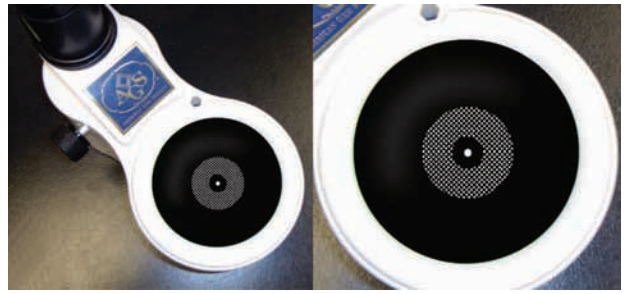

Fig. 49 Modification of the ASET instrument to display fire.

position and angular misalignment. These misalignments reduce gem symmetry and impact the illumination performance. One problem is that facet misalignment can reduce the size of the virtual facets to promote pinpoint effects at the expense of the facet interplay effect. Some light scattering can also take place at facets that do not meet as expected. Nevertheless, well-cut gems do not have significant errors to make the analysis in this paper unrealistic. For example, Fig. 51 shows a study of a real gem upon the face-up position and ±15-deg tilt position and Fig. 52 shows the same study for the corresponding perfect virtual model. Our ray-tracing methodology is discussed in Appendix C.

12 Summary of Illumination Effects

Our study is based on the actual observation of several effects that depend on the illumination conditions and on how structured illumination is produced. When a well-cut gemstone is observed and no or little light is redirected to the observer, the gemstone appears unilluminated. As broad and diffuse illumination is redirected to the observer's eyes, the stone becomes illuminated and contrast patterns take place as shown in Figs. 11 and 13. In the presence of localized sources of white light that subtend several degrees, say 3 to 12 deg, several facets across the crown become distinctly brighter. Some facets may appear lightly colored. In the presence of localized sources of white light that subtend an angle of 1 deg or less, some facets appear colored with intense colors of the visible spectrum. Facets that redirect light from localized bright sources appear as light sources themselves. Light directly reflected from the crown facets contributes glare and prevents observation of the effects taking place inside the gemstone. Upon movement of the gem, typically the tilting of the gem left to right, or tilting it backward and forward, the effects of dynamic contrast, flash and fire scintillation, and facet interplay take place. Pinpoint fire and pinpoint white flashes are also observed. The dynamic nature and the overall combination of all these effects is known as the life of the gemstone.

13 Conclusions

This paper develops a methodology for evaluating brilliance, fire, and scintillation in gemstones. The study is devoted to the round brilliant cut and the concepts and tools developed can be also applied to evaluate fancy cuts. We have highlighted the illumination effects of brilliance, contrast and dynamic contrast, fire, fire and flash scintillation, virtual facets, facet interplay, and leakage. The concept of geometrical angular spectrum has been introduced to understand how the cut and the illumination conditions impact a gem's appearance. We have developed ASET maps, fire maps, scintillation maps, and glare maps. These maps convey information about the illumination attributes of interest. The ASET maps show the ray directions that can make a gem to appear illuminated, that is, brilliant. In addition, they show how the obscuration of light by the observer's head plays an important role in creating structured illumination. We emphasize that creating structured lighting is

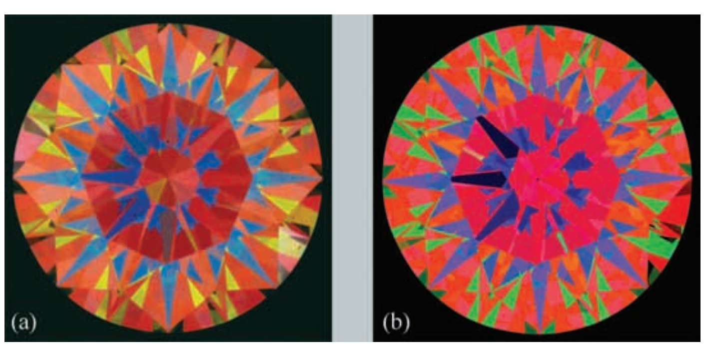

Fig. 48 Comparison of ASET photograph of a real gem (a) and the computer-generated ASET image (b).

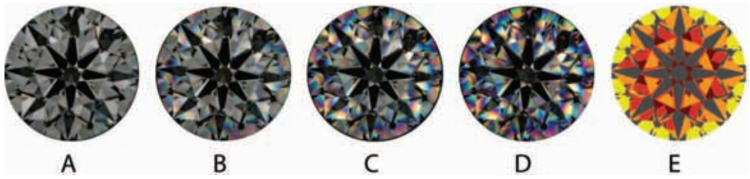

Fig. 50 Photographs of a round brilliant showing light dispersion as a function of the size of the clipping aperture. Camera *f* stops: (a) *f*/10, (b) *f*/20, (c) *f*/30, (d) *f*/40, and (e) the corresponding fire map is also shown for reference.

crucial in producing illumination appeal in gemstones. We have found out that the angular spectrum of the round brilliant cut is rich enough that, in movement, the probability of aiming at a given light source is high. Therefore and for comparison purposes, the phenomenon of fire is mainly dependent on the light dispersion produced by a gem. Thus, the fire maps that we have introduced show the potential of a given gem to exhibit fire. The scintillation maps presented show the intrinsic light scrambling properties of a given cut and simulate the appearance of a stone as it is observed. The light scrambling contributes to the creation of structured lighting and in turn to the creation of scintillation. We have divided scintillation into fire and flash scintillation.

The map matrices that are presented show upon face-up position how the illumination properties vary as a function of crown and pavilion angles. We have noted that the cutter's trade-off extends not only to brilliance properties but also to fire and scintillation properties. In particular, we introduced the anti-cutter's line where stone properties significantly change and the cutter's lines where properties are kept substantially the same. The main cutter's line contains the stones with best illumination properties. As a result of noting the cutter's trade-off, the problem of finding the best stones is simplified by one dimension in the cut space.

We have introduced tilt views along the anti-cutter's line and along the main cutter's lines that permit one to find out

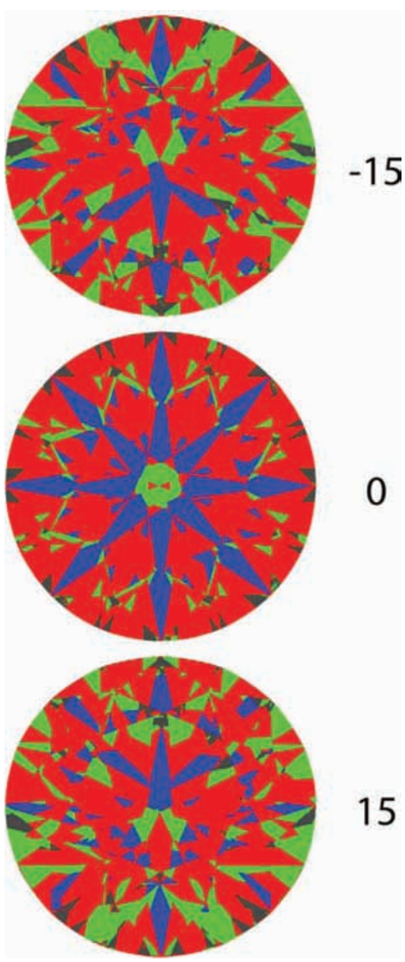

Fig. 51 Tilt study of a real gemstone at −15, 0, and +15 deg.

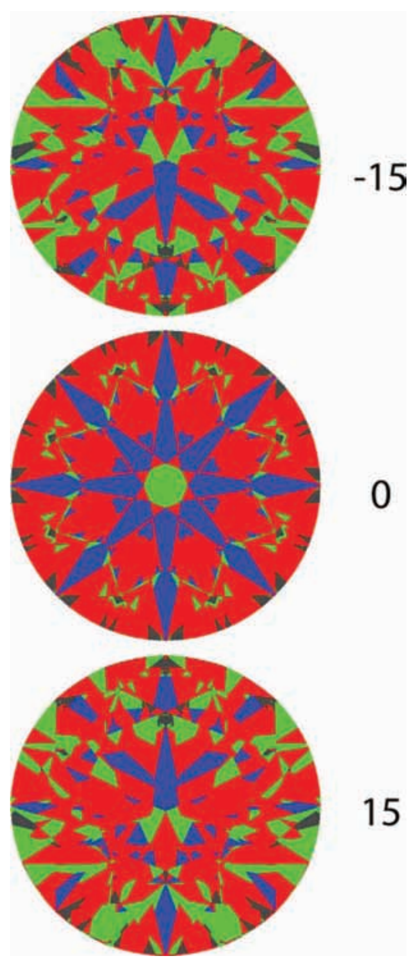

Fig. 52 Tilt study of the correspondent perfect virtual gemstone at −15, 0, and +15 deg.

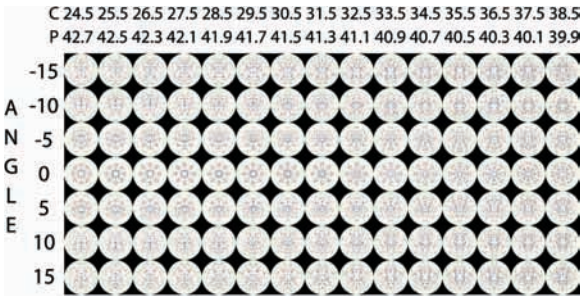

Fig. 53 Tilt view of the angular spectrum upon the primary refraction along the main cutter's line. (High-resolution image available online only. [URL: http://dx.doi.org/10.1117/1.2769018.19])

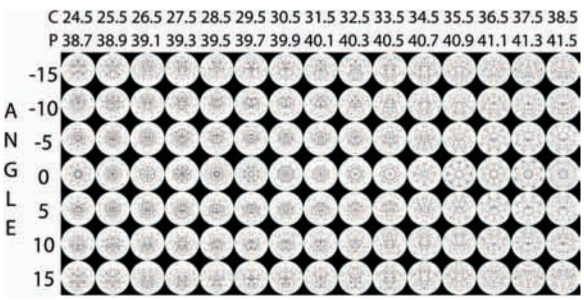

Fig. 54 Tilt view of the angular spectrum upon the primary refraction along the anti-cutter's line. (High-resolution image available online only. [URL: http://dx.doi.org/10.1117/1.2769018.20])

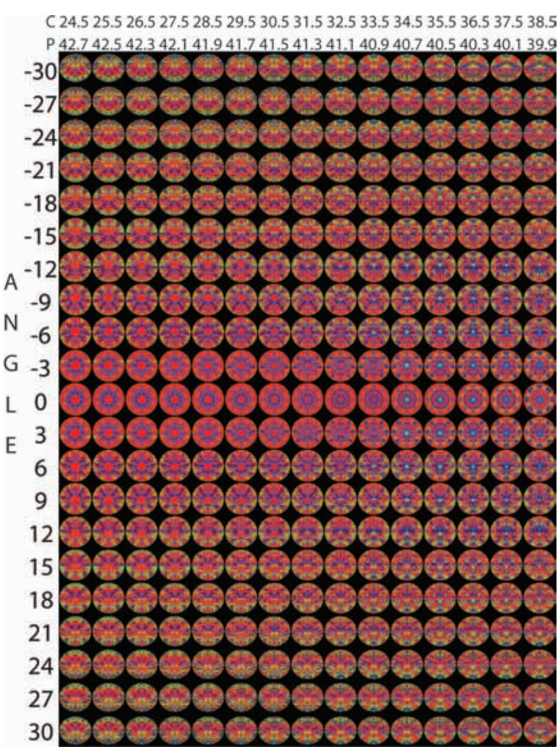

Fig. 55 Tilt view ASET maps with 40 deg of obscuration and upon the primary refraction along the main cutter's line. (High-resolution image available online only.
[URL: http://dx.doi.org/10.1117/1.2769018.21])

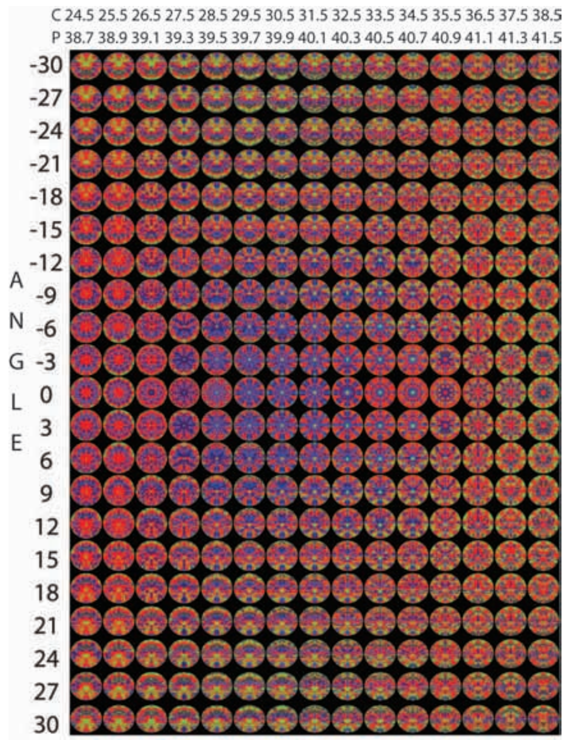

Fig. 56 Tilt view ASET maps with 40 deg of obscuration and upon the primary refraction along the anti-cutter's line. (High-resolution image available online only.
[URL: http://dx.doi.org/10.1117/1.2769018.22])

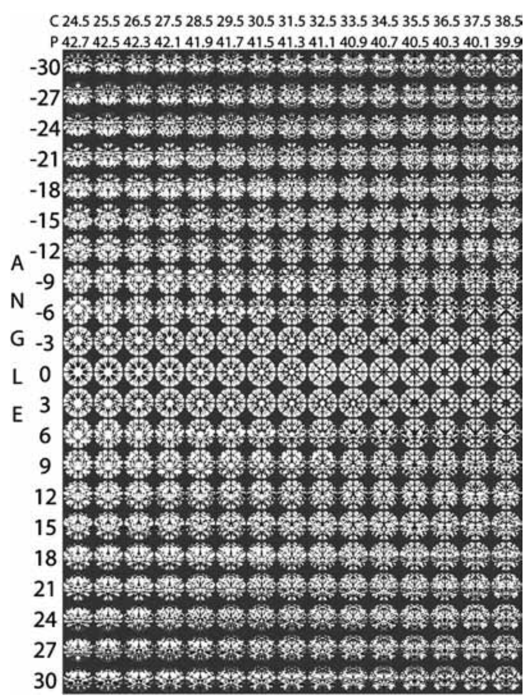

Fig. 57 Tilt view, dynamic contrast along the main cutter's line. (High-resolution image available online only. [URL: http://dx.doi.org/10.1117/1.2769018.23])

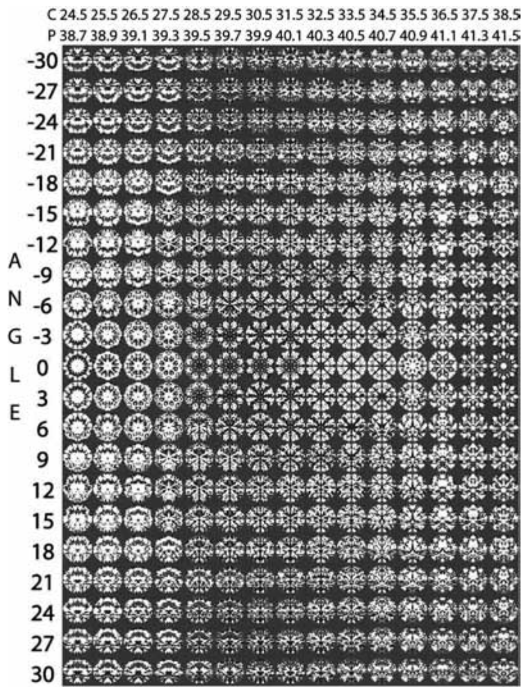

Fig. 58 Tilt view, dynamic contrast along the anti-cutter's line. (High-resolution image available online only. [URL: http://dx.doi.org/10.1117/1.2769018.24])

which is the most brilliant, the most dispersive, and the most scintillating stone. These tilt views clearly show the Tolkowsky cut as a compromise between contrast-brilliance properties and fire properties.

The maps have been generated by tracing rays in virtual gems. Quantitative data can be extracted directly from ray tracing to form metrics for gem qualitative evaluation. We have defined some metrics in terms of percentages of ray directions per crown zone, in terms of average dispersion per crown zone, and in terms of virtual facet distribution by crown zone. The value of these metrics as it refers to their ability to measure realistic illumination attributes is a subject of continued study. In addition, how the metrics are used for the purposes of gemstone grading is important and will be the subject of a future paper.

We also have developed the ASET instrument, which produces actual angular spectrum maps. These maps have a strong correlation with computer-generated maps. Of practical importance is the ray-tracing methodology that we have developed for generating the maps. Essentially, ray-tracing speed has been accelerated and the maps can be generated in a fraction of a second even though nonsequential ray tracing is involved for tracing the typically 40,000 rays needed for each map. The methodology and concepts that we have developed can also be applied for evaluating fancy cuts provided that the reduction in angular spectrum is accounted by further subdivision of the illuminating hemisphere.

Overall, we have developed understanding in the main mechanics by which gems exhibit the illumination attributes of brilliance, fire, and scintillation. We also have introduced a variety of maps that are valuable for assessing gem illumination performance. These maps are a valuable education tool in the jewelry industry. With the body of knowledge presented in this paper a gem appraiser can readily and substantially evaluate the gem attributes of brilliance, fire, and scintillation.

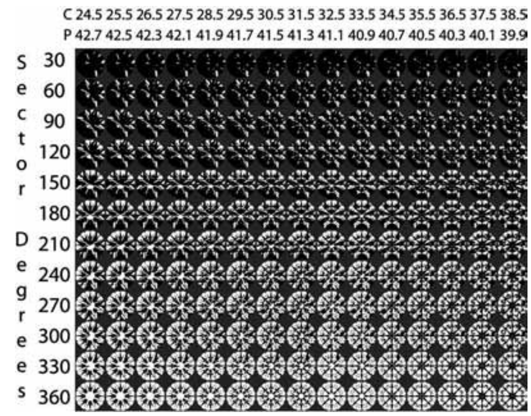

Fig. 59 Contrast around the hemisphere upon the face-up position and along the main cutter's line. (High-resolution image available online only. [URL: http://dx.doi.org/10.1117/1.2769018.25])

Appendix A: Tilt Views along the Main Cutter's Line and Anti-cutter's Line

For completeness Figs. 53–60 provide additional angular spectrum maps and tilt views.

Appendix B: Gem Specifications

Tables 1 and 2 show the specifications for a high-performance princess and emerald cut.

Appendix C: Ray Tracing

Analysis of gemstones involves nonsequential ray tracing in which an algorithm searches for the next facet to intersect after a given ray has encountered a facet. The order in which a ray intersects facets is not specified in advance but determined as the ray proceeds. This search after each ray intersection significantly slows down the ray-tracing process. Ray-tracing speed is a critical issue to render information nearly instantaneously, for real-time animations and

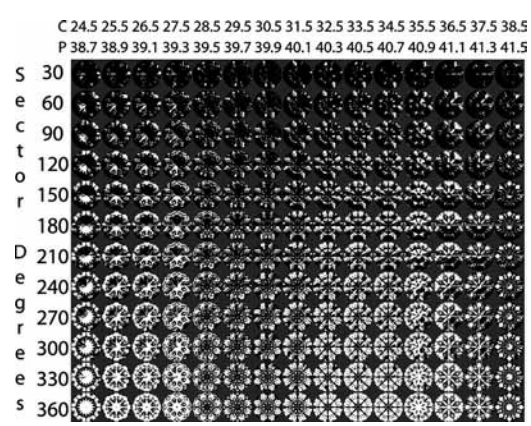

Fig. 60 Contrast around the hemisphere upon the face-up position and along the anti-cutter's line. (High-resolution image available online only. [URL: http://dx.doi.org/10.1117/1.2769018.26])

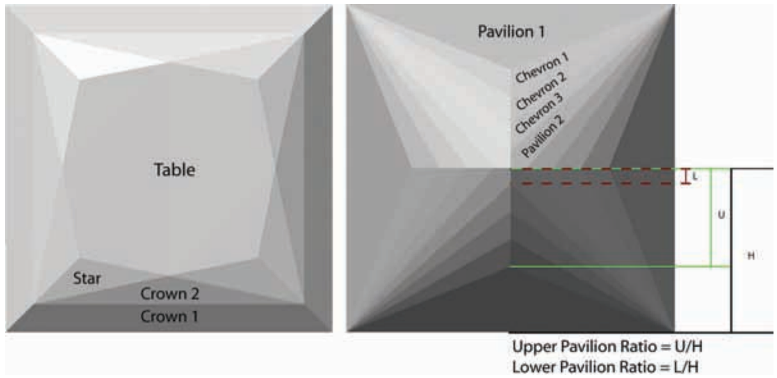

Fig. 61 High-performance princess cut and its constructional parameters.

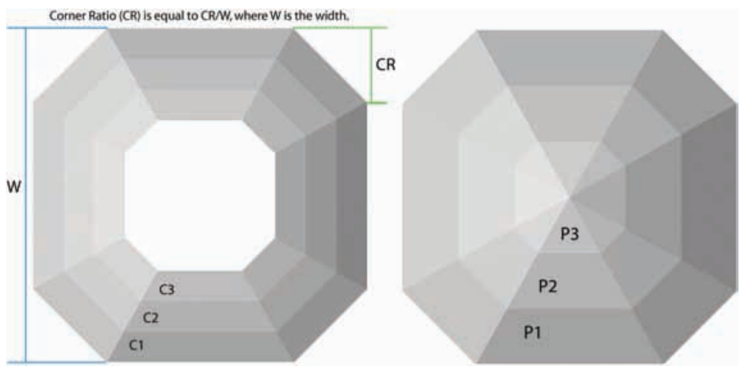

Fig. 62 High-performance emerald cut and its constructional parameters.

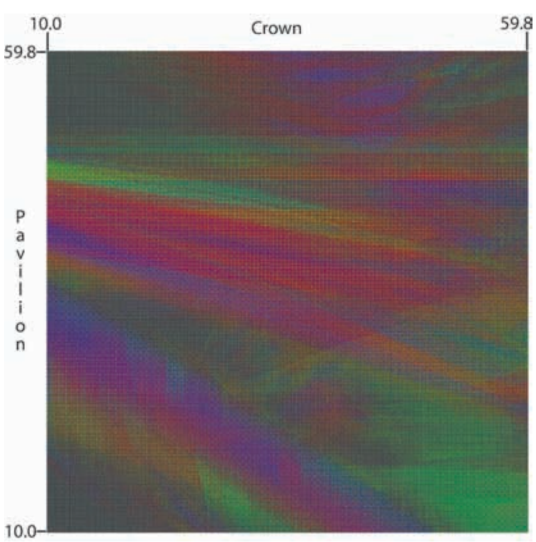

Fig. 63 Very large, very fine ASET matrix. (High-resolution image available online only. [URL: http://dx.doi.org/10.1117/1.2769018.27])

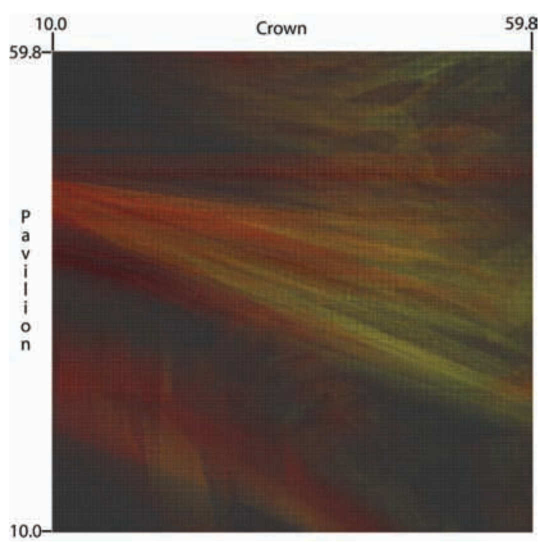

Fig. 64 Very large, very fine forward fire map matrix. (High-resolution image available online only. [URL: http://dx.doi.org/10.1117/1.2769018.28])

Table 1 Princess Cut (see Fig. 61).

Table %	Crown 1	Crown 2	Pavilion 1	Pavilion 2	Upper Pavilion Ratio[a]	Lower Pavilion Ratio[a]
66%	37.3 deg	34.5 deg	60.3 deg	39.2 deg	65%	12%

[a]The pavilion is cut with three tiers of chevron facets.

for searches through the design space. Standard nonsequential ray tracing may take tens of seconds to produce a single ASET map, which requires about 40,000 rays to achieve proper resolution. This speed is considered slow and improper for real-time animations. One way to speed up the image rendering is by the use of polygonal ray tracing where the vertices of convex regions are identified and then ray traced. This significantly reduces the number of rays that need to be traced since the interior of the polygons are painted with a color derived from vertex information. Polygonal ray tracing requires finding out how a beam of light is partitioned into polygons as it enters and propagates through a gemstone. Other issues in ray tracing gemstones are modeling and rendering.[33,34]

We have chosen not to perform polygonal ray tracing but accelerate our non-sequential ray tracing by using the concept of path memory. In this concept the path of the next ray to be traced is guessed to be the path of the previous ray, which is stored in memory. Then the ray is traced in sequential mode with the path already stored in memory. If this guess is incorrect then the ray-tracing engine assumes a nonsequential mode. By doing the ray tracing in a spiral curve, starting at the center of the gem table, it is possible to produce an ASET map in less than 1 s. The spiral curve passes by every pixel that needs to be painted with a color that depends on the information obtained by the ray trace.

A second improvement in speed results from the observation that the virtual facets of a gemstone are geometrically convex regions. That the virtual facets are convex is explained by the fact that the intersection of convex regions is also convex. That is, when a beam of light enters a gemstone it is partitioned into convex regions since the facets are convex. The partitioned convex beam remains convex as it is further partitioned by convex regions. Therefore, rather than ray tracing pixel by pixel in a spiral curve, we trace the vertex pixels in a spiral with a width of a few pixels that is divided into triangles. After proper checks, groups of pixels can be colored according to information derived from the vertices. This bears some similarity to polygonal ray tracing except that there is no need to determine how the beam is partitioned into polygons.

As an example of the use of accelerated ray tracing we present Fig. 63, which is called a very large, very fine (VLVF) dense ASET matrix. The dense matrix contains an array of 250 by 250 of individual ASET maps for the particular constructional parameters of a princess cut. The generation of a VLVF dense matrix permits one to identify regions in the cut space containing gemstones that are brilliant. By also creating a VLVF fire-map matrix, as shown in Fig. 64, and comparing it to the VLVF ASET matrix, one can look for common areas that are brilliant and fiery. The VLVF dense matrices are a valuable searching tool given that gemstone cuts have many degrees of design, which produce a large number of combinations that greatly grows with each design parameter added.

Ray-tracing at two wavelengths for fire-map creation has the problem that rays at different wavelengths may intersect different facets rather than following the same sequence of facets. To reduce this problem our Fire Maps were generated by tracing rays at wavelengths 519 nm and 521 nm and then the results were scaled to approximate the dispersion at the chosen wavelengths of 420 nm and 620 nm.

Acknowledgments

We would like to thank the American Gem Society and *JCK Magazine* for supporting this research and acknowledge the expertise that our colleagues have shared with us. Gabi Tolkowsky has shared his views about diamond beauty. Sergei Sivovolenko from Octonus and Yuri Shelementiev from the Moscow State University have shared their many years of experience in understanding illumination effects in gemstones. Martin Haske from the Adamas Gemological Laboratory has provided useful suggestions and has been a valuable critic of our methodology. Gary Holloway has raised many useful issues about diamond cutting that have impacted our views. Bruce Harding, who first determined that an observer affects the appearance of a gemstone, has provided significant help in the area of gemstone cutting. Michael Cowing from ACA Gem Laboratory has brought to our attention the importance of contrast and brightness in creating brilliance in gemstones. We thank Al Gilbertson from the Gemological Institute of America and Richard von Sternberg from EightStar Diamond Company for sharing their pioneering work about the color coding of angular ranges in gemstone evaluation. The published papers from researchers at the Gemological Institute of America provided clues and insights into gemstone appearance. The work on gemstone fire of Anton Vasiliev, from LAL Co. in Moscow, has been very helpful. Special acknowledgements are given to all diamond cutters because their insightful work in creating gemstone beauty is usually not recognized.

Table 2 Square emerald (see Fig. 62).

Table %	Corner Ratio	Crown 1	Crown 2	Crown 3	Pavilion 1	Pavilion 2	Pavilion 3
47.6%	22.9%	46.9 deg	40.0 deg	34.0 deg	47.6 deg	39.2 deg	31.2 deg

References

1. M. Tolkowsky, *Diamond Design: A Study of the Reflection and Refraction of Light in a Diamond*, Spon & Chamberlain, New York (1919), ⟨http://www.folds.net/diamond_design/index.html⟩.
2. T. Shigetomi and K. Inoue, "Device for judging brilliancy of precious stones as diamonds or the like," U.S. Patent No. 4,647,194 (1987); a description of the FireScope® is given by R. Von Sternberg, "*Today's Revolution in Diamond Cutting*," (2002), ⟨http://www.eightstar.com/images/Eightstar_Diamond.pdf⟩.
3. A. Gilbertson, "Device for judging symmetry, brightness, and efficiency of light return in precious stones," U.S. Patent No. 6,795,171 (2004); see also, A. Gilbertson *Letting Light Speak for Iitself: An Introduction to Diamond Cut Grading*, Diamond Profile, Inc., Portland, Oreg. (1998).
4. J. Sasian, P. Yantzer, and T. Tivol, "The optical design of gemstones," *Opt. Photonics News* **14**(4), 24–29 (Apr. 2003).
5. A. B. Meinel and E. S. Meinel, "Investigation of the optical behavior of brilliant cut diamonds," report to Helio Associates, Tucson, Arizona (1974).
6. B. Harding, "Faceting limits," *Gems. Gemol.* **15**(3) 78–88 (Fall 1975), ⟨http://lgdl.gia.edu/pdfs/gemsandgemology/freebackissues/fall_1975.pdf⟩.
7. B. Harding, "Diamond design revisited," ⟨http://www.gemology.ru/cut/english/tolkow2⟩.
8. J. S. Dodson, "A statistical assessment of brilliance and fire for the round brilliant cut diamond," *Opt. Acta* **25**(8), 681–692 (1978), ⟨http://www.gemology.ru/cut/english/dodson1.htm⟩.
9. GemCad software, Gemsoft Enterprises, ⟨http://www.gemcad.com⟩.
10. DiamCalc software, Octonus Co., ⟨http://www.octonus.com/oct/products/3dcalc/standard⟩.
11. ASAP, Breault Research Organization, ⟨http://www.breault.com⟩.
12. FRED, Photon Engineering, ⟨http://www.photonengr.com⟩.
13. LightTools, Optical Research Associates, ⟨http://www.opticalres.com⟩.
14. TracePro, Lambda Research, ⟨http://www.lambdares.com⟩.
15. ZEMAX, ZEMAX Development Corp., ⟨http://www.zemax.com⟩.
16. T. S. Hemphill, I. M. Reinitz, M. L. Johnson, and J. E. Shigley, "Modeling the appearance of the round brilliant cut diamond: an analysis of brilliance," *Gems. Gemol.* **34**(3), 158–183 (Fall 1998), ⟨http://www.gia.edu/gemsandgemology/18578/1945/563/back_issue_article_detail.cfm⟩.
17. I. M. Reinitz, M. L. Johnson, T. S. Hemphill, A. M. Gilbertson, R. H. Geurts, B. D. Green, and J. E. Shigley, "Modeling the appearance of the round brilliant cut diamond: an analysis of fire, and more about brilliance," *Gems. Gemol.* **37**(3), 174–197 (Fall 2001), ⟨http://www.gia.edu/gemsandgemology/18578/447/64/ back_issue_article_detail.cfm⟩.
18. S. Sivovolenko, Y. Shelementiev, and A. Vasiliev, "The results of diamond cut studies carried out in Moscow State University," (1999), ⟨http://www.cutstudy.com/cut/english/document4.htm⟩.
19. S. Sivovolenko, Y. Shelementiev, V. Onischuk, and G. Holloway, "On the problem of grading the quality of diamond cut: an analysis of some aspects of the problem," (2002), ⟨http://www.gemology.ru/cut/english/grading1/index.htm⟩.
20. M. Cowing, "Diamond brilliance: theories, measurements and judgment," *J. Gemmol.* **27**(4), 209–227 (Oct. 2000).
21. M. Cowing, "Describing diamond beauty—assessing the optical performance of a diamond," *J. Gemmol.* **29**(5/6), 274–280 (2005).
22. S. Sivovolenko, Y. Shelementiev, G. Holloway, J. Mistry, and S. Oulin, Eds., *Proc. First Intl. Diamond Cut Conf.*, Moscow, Russia, April 23–26, 2004, Russian Gemological Society, Gemological Center, Department of Geology, Main Building, Moscow State University, Leninskie Gory, GSP-2, Moscow, Russia, 119992.
23. Sarin, Sarin Technologies Ltd., ⟨http://www.sarin.com/webviewer.asp⟩.
24. Helium, Octonus Co., ⟨http://www.octonus.ru/oct/products/helium/polish⟩.
25. A. Vasiliev, "Rainbow in a colorless gem," Acta Universitatis Wratislaviensis, No. 1607, Prace geologiczno-mineralogiczne XLIV, p. 147 (1995), ⟨http://www.gemology.ru/cut/english/rainbow⟩.
26. S. Sivovolenko and Y. Shelementiev, "Different model of illumination," in *Proc. First Intl. Diamond Cut Conf.*, S. Sivovolenko, Y. Shelementiev, G. Holloway, J. Mistry, and S. Oulin, Eds., p. 48, Moscow, Russia, April 23–26, 2004, Russian Gemological Society, Gemological Center, Department of Geology, Main Building, Moscow State University, Leninskie Gory, GSP-2, Moscow, Russia, 119992.
27. Y. Kawabuchi and T. Matsumura, "Cut design of diamond for ornamental use," U.S. Patent No. 6,694,778 (2004).
28. P. Yantzer, "The effects of indexed upper half facets," ⟨http://journal.pricescope.com/Articles/15/1/The-Effects-of-Indexed-Upper-Half-Facets.aspx⟩.
29. T. Blodgett, A. Gilbertson, R. Geurts, B. Green, M. Johnson, I. Reinitz, and P. Yantzer, "Painting and digging out: variations on standard brillianteering of round brilliant diamonds," *Rapaport Diamond Rep.* **28**(21), 239–245 (2005).
30. P. Slegers, Infinity Diamonds, Private Communication (2005).
31. K. Girdharal, Inc., India, Private Communication (2006).
32. M. Haske, "Fire demonstration tool and method for using thereof," U.S. Patent Application 2005/0254037 A1.
33. S. W. Thomas, "Dispersive refraction in ray tracing," *Visual Comput.* **2**(1), 3–8 (Jan. 1986).
34. Y. Yuan, T. L. Kunii, N. Inamoto, and L. Sun, "Gemstone fire: adaptive dispersive ray tracing of polyhedrons," *Visual Comput.* **4**(5), 259–270 (Sep. 1998).

Jose Sasian is a professor at the University of Arizona, Optical Sciences College. His professional interests are in optical design, teaching optical sciences, optical fabrication, alignment and testing, telescope technology, opto-mechanics, light in gemstones, lithography, illumination optics, and light propagation.

Jason Quick received his BS degree in mathematics from MIT in 1995. He worked at MIT's Laboratory for Computer Science where he studied cellular automata and developed algorithms related to image processing and 3D graphics. Mr. Quick currently is with the R&D department at the American Gem Society Laboratories. His professional interests include computer modeling, optics, algorithm design, spectroscopy, and gemstone analysis.

Jacob Sheffield received his BA in film from UNLV in 2004. He has been with the American Gem Society Laboratories since 1999 and has worked in the R&D department since 2004. Mr. Sheffield's professional interests at the laboratory include systems analysis, computer modeling, graphic arts, and spectroscopy. In his spare time, he pursues his interests in electronic music composition, film, and other multimedia art forms.

Jim Caudill is the Director of Advanced Instruments for the American Gem Society. Prior to his current position, he worked as an analyst in the microprocessor industry for 10 years and then as a researcher at AGS laboratories from 2000 to 2004. Mr. Caudill's professional interests include engineering, scientific instrumentation, optics, photo microscopy, lecturing, and gemstone analysis. In 2007, he received certification in the LEAN Aerospace Initiative at MIT. Mr. Caudill is a professional musician/writer/producer and has performed throughout the US for over 20 years.

Peter Yantzer is the Executive Director at the American Gem Society Laboratory. Mr. Yantzer graduated in 1972 as a gemologist and was with the Gemological Institute of America from 1972 to 1979 where he served as a staff gemologist, instructor, and laboratory director. He has been with the American Gem Society Laboratory since 1995. His professional interests are in the jewelry industry, in gemstone cut technology, and gemstone grading. Mr. Yantzer received the American Gem Society's Robert M. Shipley Award in 2005.